



HAL
open science

Changes in rocky intertidal communities after the 2015 and 2017 El Niño events along the Peruvian coast

Juan Valqui, Bruno Ibañez-Erquiaga, Aldo S Pacheco, Lynn Wilbur, Diana Ochoa, Jorge Cardich, Maria Pérez-Huaranga, Rodolfo Salas-Gismondi, Alexander Pérez, Aldo Indacochea, et al.

► To cite this version:

Juan Valqui, Bruno Ibañez-Erquiaga, Aldo S Pacheco, Lynn Wilbur, Diana Ochoa, et al.. Changes in rocky intertidal communities after the 2015 and 2017 El Niño events along the Peruvian coast. Estuarine, Coastal and Shelf Science, 2021, 250, pp.107142. 10.1016/j.ecss.2020.107142 . hal-03196027

HAL Id: hal-03196027

<https://hal.science/hal-03196027v1>

Submitted on 14 Dec 2021

HAL is a multi-disciplinary open access archive for the deposit and dissemination of scientific research documents, whether they are published or not. The documents may come from teaching and research institutions in France or abroad, or from public or private research centers.

L'archive ouverte pluridisciplinaire **HAL**, est destinée au dépôt et à la diffusion de documents scientifiques de niveau recherche, publiés ou non, émanant des établissements d'enseignement et de recherche français ou étrangers, des laboratoires publics ou privés.

Changes in rocky intertidal communities after the 2015 and 2017 El

Niño events along the Peruvian coast

Juan Valqui^{1,2}, Bruno Ibañez-Erquiaga^{3,4}, Aldo S. Pacheco⁵, Lynn Wilbur^{6,7}, Diana Ochoa¹,
Jorge Cardich¹, Maria Pérez-Huaranga¹, Rodolfo Salas-Gismondi^{1,8,9}, Alexander Pérez¹, Aldo
Indacochea¹⁰, Jose Avila-Peltroche¹¹, Maria Rivera Ch¹, Matthieu Carré^{1,12*}

¹ Laboratorios de Investigación y Desarrollo (LID)-Facultad de Ciencias y Filosofía and Centro de
Investigación para el Desarrollo Integral y Sostenible (CIDIS), Universidad Peruana Cayetano
Heredia, Lima, Peru

² Centro de Ornitología y Biodiversidad CORBIDI, Lima, Perú

³ Departamento de Química y Biología, Universidad San Ignacio de Loyola, Lima, Perú

⁴ Asociación CONSERVACCION, Lima, Perú

⁵ Facultad de Ciencias Biológicas, Universidad Nacional Mayor de San Marcos, Lima, Perú

⁶ Oceanlab, Department of Zoology, University of Aberdeen, UK

⁷ Marine Alliance of Science and Technology Scotland (MASTS), Scottish Oceans Institute

St. Andrews, UK

⁸ Division of Paleontology, American Museum of Natural History, NY, USA

⁹ Departamento de Paleontología de Vertebrados, Museo de Historia Natural, Universidad Nacional
Mayor de San Marcos, Lima, Perú

¹⁰ Laboratorio de Ecología Marina, Facultad de Ciencias Veterinarias y Biológicas, Universidad
Científica del Sur, Perú

1
2
3
4
5
6
7
8
9
10
11
12
13
14
15
16
17
18
19
20
21
22
23
24
25
26
27
28
29
30
31
32
33
34
35
36
37
38
39
40
41
42
43
44
45
46
47
48
49
50
51
52
53
54
55
56
57
58
59
60
61
62
63
64
65

¹¹ Department of Life Science, Chosun University, Gwangju, South Korea

¹² LOCEAN Laboratory, Sorbonne Universités (UPMC)-CNRS-IRD-MNHN, Paris, France

*** Corresponding author:**

Matthieu Carré, matthieu.carre@locean.ipsl.fr

Keywords: Humboldt current ecosystem, Macrobenthos, Biogeography, Community structure, Thermal anomaly, latitudinal pattern

Highlights

- Rocky intertidal communities' response to El Niño in a latitudinal transect
- Community changes driven by ecological processes rather than thermal tolerance
- Biogeographical patterns are persistent to El Niño

Abstract

The Peruvian coast experiences the largest interannual variability of sea surface temperature in the world due to the combined influence of the coastal upwelling and El Niño Southern Oscillation (ENSO). Although biological impacts of El Niño events have been widely reported, their effects on rocky intertidal communities remains largely unknown in Peru. Herein, we analyze the results of two biological surveys of rocky intertidal communities, conducted along 1400 km of the Peruvian coast. The first survey was conducted in 2015 yielding a snapshot of the distribution of rocky intertidal communities after 17 years of stable La Niña-like conditions. The second survey was carried in

1
2
3 44 October 2017, after the 2015-16 and the 2017 El Niño events, which produced warm sea surface
4
5 45 temperature (SST) anomalies up to 6°C on the Peruvian coast. We find no changes throughout the
6
7
8 46 latitudinal transect in taxonomic richness but an important turnover of species, especially marked in
9
10 47 the transition zone (~4-8°S) between the Panamic and the Humboldt provinces. Temperature-related
11
12
13 48 southward migration of species was evidenced in a few sites but did not explain the large-scale
14
15 49 change in communities observed from 2015 to 2017, primarily driven by large changes in the
16
17
18 50 distribution of a few ecologically important species across the Panamic and Humboldt provinces. A
19
20 51 primary environmental impact on some ecologically key species likely triggered a chain of secondary
21
22 52 impacts through ecological relationships which lead to a complex change independent from SST
23
24
25 53 gradients. Further studies are needed to better characterize and disentangle the seasonal and
26
27 54 interannual variability of the rocky intertidal communities and their drivers. When this interannual
28
29
30 55 variability is integrated, the nine study sites show a highly persistent community structure determined
31
32 56 by the latitudinal SST gradient along the Peruvian coast.
33
34
35 57

38 58 **1. Introduction**

39
40 59 El Niño Southern Oscillation (ENSO) is responsible for approximately 85% of the interannual
41
42 60 climatic variability along the Peruvian coast (Carré *et al.*, 2013). El Niño, the warm phase of ENSO,
43
44 61 generates sea surface temperature (SST) anomalies that are larger in Peru than anywhere else in the
45
46 62 world, with widespread effects on marine ecosystems. During ENSO-neutral conditions of oceanic
47
48 63 circulation and considering the low latitude, coastal waters are relatively cold (16-20°C) due to
49
50 64 coastal upwelling. During El Niño events, the thermocline deepens in the Eastern Pacific preventing
51
52 65 the upwelling of deeper cold and nutrient-rich waters to the surface. As a result, primary productivity
53
54 66 is reduced and SST increases considerably between 3 to 18 months depending on the magnitude of
55
56 67 the event (Wyrтки, 1975; Cane, 1983). Temperature anomalies can reach up to 8°C during extreme
57
58
59
60
61
62
63
64
65

1
2
3 68 events like those that occurred in 1982/83 and 1997/98 (Carré *et al.*, 2013). These interannual marine
4
5 69 temperature anomalies are the largest in the world and, coupled with others abiotic cofactors (e.g.,
6
7
8 70 rainfall and salinity changes), can have significant impacts on the coastal biodiversity either directly
9
10 71 or indirectly (Barber and Chavez, 1983; Paredes *et al.*, 1998; Espino, 1999; Arntz *et al.*, 2006;
11
12 72 Camus, 2008). The opposite phase of ENSO referred to as La Niña, is characterized by cooler
13
14
15 73 conditions related to a shallower thermocline and an intensification of the coastal upwelling. These
16
17
18 74 cold anomalies have lower amplitude, favor primary productivity, and are generally not considered as
19
20 75 stressful conditions for the coastal Peruvian ecosystem (Wang and Fiedler, 2006).

21
22 76 To date, no continuous, periodic and comparable observations of rocky shores biological
23
24
25 77 communities along the Peruvian coast and continental margin are available. Several studies document
26
27 78 the biological effects of El Niño in Peruvian coastal ecosystems during the extreme 1982-83 and the
28
29
30 79 1997-98 events (Arntz, 1986; Glynn, 1988; Castilla and Camus, 1992; Arntz *et al.*, 1988; Tarazona *et*
31
32 80 *al.*, 1988a; Tarazona *et al.*, 1988b; Tarazona *et al.*, 2003; Thiel *et al.*, 2007; Camus, 2008) but focus
33
34
35 81 on site specific variability. Information about the influence of ENSO on rocky intertidal benthic
36
37 82 fauna and flora in Peru is thus scarce and has never been investigated along a latitudinal gradient.

38
39 83 Recently, Ibañez-Erquiaga *et al.* (2018) proposed a biogeographic zonation of rocky intertidal
40
41
42 84 communities along the Peruvian coast based on a latitudinal survey performed from February to May
43
44 85 2015 in 41 coastal sites. The authors defined three biogeographic units: (1) a tropical, Panamic
45
46
47 86 province (3.5 - 4.5° S), (2) a transitional zone (5 - 5.5° S), and (3) a temperate, Humboldt province (6
48
49 87 - 13.5°S). The model proposed by Ibañez-Erquiaga *et al.* (2018) provides a snapshot of the latitudinal
50
51
52 88 distribution of rocky intertidal communities after 17 years of relatively cool and stable La Niña-like
53
54 89 conditions after the strong 1997-98 El Niño event. Herein, we add data from a survey performed in
55
56
57 90 October 2017 at 9 sites (among those sampled by Ibañez-Erquiaga *et al.*, 2018) distributed along
58
59 91 1400 km of the Peruvian coast (from 3.7 to 13.9° S) (Figure 1). Thus, we assumed that ecosystems

1
2
3 92 had fully recovered from the 1998 El Niño disturbance and were under the long-term influence of La
4
5 93 Niña conditions in Peru.
6
7
8 94 Two El Niño events occurred between surveys. The 2015-16 El Niño is considered among the most
9
10 95 powerful of the last decade (Huang *et al.*, 2016), with a maximum anomaly located in the central
11
12 96 Pacific region and a moderate warming in the Eastern tropical Pacific and in the Peruvian coast
13
14
15 97 (Figure 2). Soon after, a short-lasting El Niño event occurred from January to May 2017 (known as
16
17 98 coastal El Niño), characterized by a much larger temperature anomaly but restricted to the coast off
18
19
20 99 Peru and Ecuador (Echevin *et al.*, 2018; Garreaud, 2018). In central Peru, SST anomalies reached 6°
21
22 100 C (Figure 2) and together with catastrophic rainfall and floods across the coast (Rodríguez-Morata *et*
23
24 101 *al.*, 2018). Although not as severe as the extreme 1982-83 and 1997-98 events, the 2017 coastal El
25
26
27 102 Niño event has been considered as a strong but localized event for the amplitude of the temperature
28
29
30 103 anomaly on the Peruvian coast (Echevin *et al.*, 2018; Garreaud, 2018). Our second survey was
31
32 104 conducted in October, about 4 months after the end of this event. Therefore, this second survey is
33
34
35 105 ideal to assess long-lasting impacts of El Niño environmental variability in biological communities
36
37 106 after a long period of being predominantly under rather cool neutral or La Niña conditions.
38
39 107 Ibañez-Erquiaga *et al.* (2018) showed that temperature and nutrients are strongly linked with the
40
41
42 108 biogeographic zonation of benthic rocky communities. Since surface warm water masses are also
43
44 109 characterized by low nutrient concentration, here we use SST anomalies as an integrated indicator of
45
46
47 110 the oceanographic state on the Peruvian coast. We expected long-lasting impacts of El Niño on the
48
49 111 rocky shore communities including changes in the species diversity and in the latitudinal pattern of
50
51
52 112 community composition due to mortality, southward migration, and a southward shift in species
53
54 113 recruitment.
55
56 114 The objective of this study is twofold. First we aimed to evaluate the cumulative impact of the 2015-
57
58
59 115 16 and 2017 El Niño events on species diversity and geographic distribution of benthic rocky
60
61 116 intertidal communities across the Peruvian Pacific coast, by assessing changes in the characteristics
62
63
64
65

1
2
3 117 and latitudinal patterns in the communities before and after the El Niño events in relationship with
4
5 118 SST anomalies along the coast. Because earlier systematic records of rocky shore communities are
6
7
8 119 not available in Peru, our approach lacks referential observations, but is also the first study of rocky
9
10 120 intertidal communities' response to El Niño in a latitudinal transect. Our second aim was to assess
11
12
13 121 the robustness of the bioregionalization to inter-annual variability, as well as the relative influence of
14
15 122 mean SST conditions versus El Niño-related SST anomalies as long-term abiotic drivers of the
16
17
18 123 biogeographic zonation of rocky intertidal species along the Peruvian coast, comparing the
19
20 124 biogeographic zonation of rocky shore communities with latitudinal gradients in long-term statistics
21
22 125 of coastal SST including ENSO-related variability.
23
24
25 126

28 127 **2. Materials and Methods**

31 128 **2.1. Study area, site selection and sampling design**

34 129 We studied nine rocky shore sites of the Peruvian coast, from Acapulco (3.74° S, 80.77° W) to La
35
36 130 Mina (13.91° S, 76.31° W) encompassing a 1400 km stretch of coastline (1200 km in direct line), or a
37
38
39 131 variation of 11.63° latitude and 6.14° longitude (Figure 1). These nine sites were selected among the
40
41 132 41 sites survey performed between February and May of 2015 by Ibañez-Erquiaga *et al.* (2018)
42
43
44 133 allowing a direct comparison in these localities. Sites were separated by 0.5 to 2.8° of latitude with a
45
46 134 shorter distance between northern sites where gradients are steeper and where the transition between
47
48
49 135 the Panamic and the Humboldt ecoregion was reported (Figure 1, Table 1). Fishing, recreational, or
50
51 136 urban areas were avoided to minimize the anthropogenic influence in community composition.
52
53
54 137 Selected sites were rocky shore, with wave-exposed platforms from 25 m² to ~1000 m². The slope of
55
56 138 the rock platform did not exceed 45°. Caves and crevices were not surveyed to keep a homogeneous
57
58
59 139 flat sampling area. At each site, observations were performed in a representative sample of the
60
61 140 intertidal zone through a total of 16 quadrats distributed in four haphazardly-distanced (in a range of
62
63
64
65

1
2
3 141 3-10m) transects of four quadrats distributed from the upper intertidal to the lower intertidal zones.
4
5 142 We used a 0.25 m² quadrat of 0.50 m x 0.50 m with a 100-intersection grid. In each transect 4
6
7
8 143 intertidal fringes were identified according to the presence of litorinids (upper), sessile barnacles
9
10 144 (mid-high), mussels (mid-low) and macroalgae and anemones (low) following the sampling method
11
12
13 145 presented in Broitman *et al.* (2001), Rivadeneira and Fernandez (2005) and Ibañez-Erquiaga *et al.*
14
15 146 (2018). Within each fringe and along the transect, one quadrat was randomly placed on plain rock
16
17
18 147 surface. We used a 0.25 m² quadrat of 0.50 m x 0.50 m with a 100-intersection grid. Each site
19
20 148 sampling cover thus a total surface area of 4 m² and 1600 point-intersects, which is similar to
21
22
23 149 previous rocky shore studies in the Pacific (Broitman *et al.*, 2001; Blanchette *et al.*, 2008;
24
25 150 Rivadeneira and Fernandez, 2005; Ibañez-Erquiaga *et al.*, 2018). Sampling was conducted during the
26
27 151 lowest tide at daytime and lasted about 3 hours per site.
28
29

30 152

33 153 **Table 1.** Study sites coordinates and sampling dates

Site name	Sitecode	Latitude °N	Longitude °E	1 st sampling	2 nd sampling
Acapulco	ACA	-3.74	-80.77	22/02/2015	2/10/2017
PuntaVeleros	PVE	-4.17	-81.14	21/02/2015	6/10/2017
PuntaBalcones	PBA	-4.68	-81.32	1/03/2015	5/10/2017
Yacila	YAC	-5.12	-81.16	3/03/2015	3/10/2017
PuntaAguja	PAG	-5.80	-81.08	15/03/2015	4/10/2017
Puemape	PUE	-7.51	-79.54	10/03/2015	7/10/2017
Tamborero	TAM	-10.32	-78.05	8/04/2015	8/10/2017
Pucusana	PUC	-12.47	-76.79	17/04/2015	13/10/2017
La Mina	MIN	-13.91	-76.31	8/05/2015	18/10/2017

50 154

51
52
53 155 The zonation pattern for the region sampled has been described in Paredes (1974) for the central
54
55 156 coast, and further characterized by Ibanez-Erquiaga *et al.* (2018). These authors describe for the
56
57
58 157 rocky intertidal of the Panamic Province, the predominance of *Jehlius cirratus* and *Austrolittorina*
59
60 158 *araucana* for the upper intertidal level, *Ulva* spp. for the middle level, and *Semimytilus algosus* with
61
62
63
64
65

1
2
3 159 *Grateloupia filicina* in the low level. In the Transition Zone, *J. cirratus* and *Echinolittorina* spp. are
4
5 160 predominant in the upper intertidal level, *Ulva* spp. and *Phragmatopoma* spp. characterize the middle
6
7
8 161 level, and *G. filicina* with *Ahnfeltiopsis durvillaei* are predominant in the lower level. For the
9
10 162 Humboldt ecoregion, *J. cirratus* and *Echinolittorina* spp. are predominant in the upper intertidal
11
12
13 163 level, *Perumytilus purpuratus* and *Ulva* spp. characterize the middle level, and *S. algosus* the lower
14
15 164 level.

16
17
18 165

21 166 **2.2. Data collection at the rocky intertidal habitat**

22
23
24 167 A commonly used minimum size of 0.5 cm was chosen as size limit for individuals to be counted.
25
26 168 Mobile species (e.g. limpets, snails, crabs, mobile polychaetes) were counted as individuals present
27
28
29 169 within the quadrats (4m² in total), and their abundance was reported in number of individuals per
30
31 170 square meter. The abundance of sessile species (e.g. mussels, barnacles, algae, anemones, sessile
32
33
34 171 polychaetes) was measured as a percentage of coverage using a 100-point grid within quadrats (1600
35
36 172 intercept points in total). Percentage of rocky and sandy substratum was also quantified. When full
37
38
39 173 taxonomic identification was not achieved *in situ*, specimens were collected in 96% alcohol
40
41 174 (invertebrates) or 4% formalin (algae) for further examination in the laboratory. Some genera include
42
43
44 175 species that cannot be differentiated visually in the field, such as *Scurria* or *Ulva*, which means that
45
46 176 their identification and quantification in the laboratory would require the collection of all individuals
47
48 177 in the field. This option was not chosen because of its high environmental impact, so that these
49
50
51 178 genera are not resolved here to the species level. *Scurria* species have been shown to be separated by
52
53 179 small scale processes rather by large scale biogeographic features (Aguilera et al. 2013), so that this
54
55
56 180 taxonomic limitation is not expected to induce any significant bias in our study. Collected samples
57
58 181 were deposited at the collection of the Marine Biology Laboratory of the Universidad Peruana
59
60
61 182 Cayetano Heredia in Lima, Peru. In the laboratory, a stereoscope or microscope was used to sort
62
63
64
65

1
2
3 183 specimens into major taxa and then identified to the lowest possible taxonomic level. When possible,
4
5 184 Holothurian ossicles were extracted and observed to identify to the species level. Where the
6
7
8 185 taxonomic uncertainty persisted, species were pooled into genera. Taxonomic identification was
9
10 186 double checked for consistency.
11
12

13 187
14
15

16 188 **2.3. Temperature data**

17
18

19 189 Sea surface temperature (SST) data was obtained from the Multi-scale Ultra-high Resolution (MUR)
20
21 190 SST Analysis fv04.1, Global, 0.01°x0.01° (Vazquez *et al.*, 1998; JPL MUR MEaSURES Project,
22
23
24 191 2015). The monthly time series covers the period from June 2002 to April 2018. This dataset was
25
26 192 chosen because coastal features can be captured by the ultra-high spatial resolution of ~1 km. In
27
28
29 193 figure 3, we show maps of (A) mean annual SST, (B) annual SST range, (C) mean July SST, (D)
30
31 194 mean February SST, and (E) the influence of ENSO estimated by the variance (squared standard
32
33
34 195 deviation) of SST anomalies. SST statistics were calculated over the 2002-2018 period. Monthly
35
36 196 anomalies were calculated in reference to the 2003-2016 period. For all these variables, the trend
37
38
39 197 observed along the coastline was plotted vs. latitude. Monthly time series of SST anomalies
40
41 198 calculated for each sampling sites are shown in figure 2. The map of SST anomalies observed in
42
43 199 March 2017 (Figure 3F) shows the spatial pattern of the maximum temperature stress of the 2017
44
45
46 200 Coastal El Niño event.
47
48

49 201
50
51

52 202 **2.4. Data analysis**

53
54

55 203 A sampled based rarefaction analysis (Gotelli and Colwell, 2001) was performed to assess the
56
57 204 sampling representativeness for the nine sampled localities. Taxa composition (presence/absence),
58
59
60 205 abundance (number of individuals per square meter for mobile species, or percentage of coverage for
61
62
63
64
65

1
2
3 206 sessile species) and the Chao2 estimator of species richness (Chao et al., 2009) were calculated for
4
5 207 each site and each survey. Chao2 index values were calculated with presence/absence data of all taxa
6
7
8 208 using the R package SpadeR (Chao et al., 2016).
9
10
11 209 Non-metric multi-dimensional scaling (nMDS) was used to build ordination plots calculated from the
12
13 210 Sorensen-Dice similarity matrices. The nMDS analyses were conducted with the presence-absence
14
15
16 211 data set of sessile and mobile species using the R package 'vegan' (Oksanen *et al.*, 2010). The nMDS
17
18 212 analysis was first applied to the full 2015 presence/absence dataset (41 sites) together with the 2017
19
20
21 213 dataset (9 sites) to assess the dissimilarity between these two periods and test if the samples from
22
23 214 2017 fit in the 2015 latitudinal pattern. The same analysis was repeated without singletons (taxa that
24
25 215 have been recorded in only one site and one year) to assess the effect of rare species (Supplementary
26
27
28 216 information). The difference between abundance data and presence-absence data in the sites surveyed
29
30 217 in 2015 and 2017 was calculated to detect species with large changes in their abundance or spatial
31
32
33 218 distribution (Tables S1 and S2). We evaluated the median latitude of the distribution before and after
34
35 219 the El Niño events for each species observed both in 2015 and 2017. We compared median latitudes
36
37
38 220 in 2015 to those observed in 2017 using a paired t-test to assess a potential latitudinal shift in species
39
40 221 distributions.
41
42
43 222 Observations of 2017 were then combined with those obtained in 2015 in the same sites to test
44
45 223 whether the biogeographical zonation is robust to interannual variability. A second nMDS analysis
46
47
48 224 was performed for the combined dataset using the same methodology (Bray–Curtis similarity
49
50 225 matrices using presence-absence data). The influence of temperature on the rocky intertidal
51
52
53 226 biogeography was evaluated by least square linear regressions between the principal axis of this
54
55 227 second nMDS ordination and SST statistics calculated over the 2002-2018 period (annual mean,
56
57
58 228 February mean, July mean, and the variance of SST anomalies).
59
60
61
62
63
64
65

1
2
3 229 A power analysis was performed using the G*Power 3.1 software (Faul et al., 2009) when no
4
5 230 correlation was detected between two variables. Post hoc evaluations were performed for bivariate
6
7
8 231 regression assuming normal distribution, using a 0.05 α significance level, and correlation coefficient
9
10 232 $R = 0$ as null hypothesis. We report $R_{P0.8}$, the minimum value of the true correlation coefficient so
11
12 233 that the dataset statistical power is above 0.8. In other words, $R_{P0.8}$ represents the correlation
13
14
15 234 coefficient that the dataset can reject with a type II error probability less than 0.2, which is the
16
17
18 235 recommended threshold in statistical power analysis (Peterman, 1990). We also report the achieved
19
20 236 post-hoc power.

21
22
23 237 Linear correlations were tested for spatial autocorrelation by evaluating the significance of the
24
25 238 Moran's I coefficient through Monte Carlo and normal distribution (Supplementary information).
26
27
28 239 When strong autocorrelations were found, generalized least squares (GLS) models were calculated so
29
30 240 the influence of the spatial structure was incorporated into the linear regression model through the
31
32
33 241 residual terms (Diniz-Filho et al., 2003). Different correlation spatial structures were tested, and the
34
35 242 best fitting model was defined using the lowest Akaike Information Criterion (AIC) along with the
36
37
38 243 less negative Log-Likelihood (LogLik) values (Supplementary information). Finally, a cluster
39
40 244 analysis using Sorensen-Dice index was performed, using the software 'PAST' (Hammer *et al.*,
41
42 245 2000), to study the similarity between study sites using presence-absence data of mobile and sessile
43
44
45 246 species. Robustness of tree topologies was assessed through 10000 bootstrap replications. All
46
47 247 statistics, except when noted, were done using R 3.5.0 (R-Core Team, 2018), through the *spdep*
48
49
50 248 (Bivand et al., 2013), *nlme* (Pinheiro et al., 2018), and *MuMIn* (Barton, 2020) packages.

51 52 53 249 54 55 250 **3. Results**

56
57
58 251 Sites are listed in table 1 and hereafter referred to in the text and figures by their acronym and
59
60 252 latitude. The 2017 dataset is composed of 1076 observations (an observation being the
61
62
63
64
65

1
2
3 253 documentation of the presence of any given species within a set quadrat) resulting in 79 taxa, while
4
5 254 924 observations, resulting in 69 taxa were obtained in the same sites in 2015. Due to spring tides,
6
7
8 255 hazardous swell or other logistic constrains, data from 13 quadrats (1 in PVE[4.17°S], 3 in
9
10 256 TAM[10.32°S], and 8 in PUC[12.47°S], representing 9.0% of the sampled surface) in 2015 and data
11
12
13 257 from one quadrat (PBA[4.68°S], representing 0.7 % of the sampled surface) in 2017 could not be
14
15 258 sampled. Observations obtained in 2015 and 2017 for the nine analyzed sites are reported in the
16
17
18 259 online supplementary data Table S1 as abundance data and in Table S2 as presence/absence data. The
19
20 260 complete 2015 dataset (41 sites) is available online in Ibañez-Erquiaga *et al.* (2018). Sampled-based
21
22 261 rarefaction analysis showed that the number of taxa is reasonably close to the asymptotic maximum
23
24
25 262 in the nine locations and both surveys, indicating that sampling effort was enough for obtaining an
26
27 263 acceptable representation of the taxonomic richness (Figure 4), thus supporting the validity of the
28
29
30 264 following analyses.

31 32 33 265 **3.1. Species incidence and abundance**

34
35 266 In this study 104 taxa were identified, of which 79 were identified to the species level. 40 species
36
37
38 267 were observed only once in the 9 study sites.

39
40
41 268 The most abundant sessile species was the barnacle *Jehlius cirratus* (19.5% of total coverage in 2015
42
43 269 and 13.6% in 2017). Other species with high abundance include the green algae *Ulva* spp., and the
44
45
46 270 encrusting algae *Lithophyllum* spp.. The most abundant mobile species were the periwinkle
47
48 271 *Echinolittorina* spp. (accounting for 46.8% of total abundance in 2015 and 24.3% in 2017, reaching
49
50
51 272 top densities of 521.3 individuals per m² in TAM[10.3°S] in 2015, the limpet *Scurria* spp.. The
52
53 273 periwinkle *Austrolittorina araucana*, highly abundant and characteristic of the upper intertidal zone
54
55
56 274 in 2015 had disappeared in these sites in 2017 (Table S1).

57
58 275 Among the 24 most abundant taxa (each representing over 1% of the total abundance or coverage), a
59
60
61 276 majority was ubiquitous: *Echinolittorina* spp., *Jehlius cirratus*, *Scurria* spp., *Ulva* spp., *Tegula* spp.,
62
63
64
65

1
2
3 277 *Lithophyllum* spp., *Corallina officinalis*, encrusting brown algae. The anemone *Oulactis concinnata*
4
5 278 was the most abundant sessile species in the two northernmost sites ACA[3.7°S] and PVE[4.2°S].
6
7
8 279 Taxa with high abundance and only occurring in the Humboldt province include the mussel
9
10 280 *Perumytilus purpuratus*. Taxa with high abundance occurring only in the transition zone were the
11
12
13 281 snail *Stramonita haemastoma* and the red algae *Gelidium pusillum*.
14
15
16 282
17
18
19 283 We now report changes in taxa presence, abundance, and distribution between 2015 and 2017. 44
20
21 284 taxa have been identified both in 2015 and 2017. 25 taxa were observed in 2015 in those sites but not
22
23 285 in 2017, while conversely, 35 taxa were only observed in 2017. Among those 60 taxa that appeared
24
25
26 286 or disappeared, most (65%) are rare (observed only once). However, some of them, were widespread
27
28 287 and/or abundant in one of the surveys.
29
30
31 288 Among the taxa that disappeared, 3 were widespread in 2015. The most notorious is *Austrolittorina*
32
33
34 289 *araucana*, abundant in all sites of the northern and central coast of Peru in 2015 in the upper
35
36 290 intertidal zone. The macroalgae *Grateloupia filicina*, abundant in 2015 in the central coast, from 5 to
37
38
39 291 10°S, was not observed in 2017. The snails *Diloma nigerrimum* and *Prisogaster niger*, present in
40
41 292 2015 in the southern sites, disappeared in 2017. *Polysiphonia* spp. observed in 3 sites at different
42
43 293 latitudes in 2015 was absent in 2017. Important taxa whose distribution was strongly reduced in 2017
44
45
46 294 include the limpet *Siphonaria* spp. which disappeared from 5 sites but curiously appeared in great
47
48 295 abundance in 2017 in PAG[5.8°S]. The algae *Gymnogongrus durvillei*, the anemone *Phymanthea*
49
50
51 296 *pluvia*, and the mussel *Semimytilus algosus* disappeared from 4 sites, which shifted their distribution
52
53 297 southward by 4.8°, 6.4°, and 1.8° of latitude, respectively. *Jehlius cirratus*, the most abundant sessile
54
55
56 298 species of the Peruvian rocky shores, showed a decreased coverage in most sites in 2017.
57
58
59 299 The 2017 survey also showed remarkable increases in some taxa. 4 taxa appeared in 3 to 6 sites in
60
61 300 2017: the snails *Mitrella baccata* and *Stramonita biserialis* in the northern sites, the cucumber
62
63
64
65

1
2
3 301 *Patallus mollis* in the south, and the sea anemona *Phymactis clematis* from 4.7° to 13.9°S. *Fissurella*
4
5 302 spp., restricted to 2 northern sites in 2015, spread in 5 sites down to the southernmost site. The chiton
6
7
8 303 *Acanthopleura echinata* was observed in 3 more sites. The limpet *Scurria spp.*, as well as the algae
9
10 304 *Corallina officinalis* and the encrusting brown algae (possibly *Ralfsia sp.*) became more widespread
11
12
13 305 and abundant and tend to expand their distribution northward.
14
15 306 We thus observe that some taxa shifted their distribution southward while others shifted northward.
16
17
18 307 The average latitudinal shift (estimated by the change in the median latitude of taxa presence) of all
19
20 308 taxa is not significant (t-test). Among the 9 main taxa that showed an increased abundance and
21
22
23 309 distribution, 6 are mobile and 3 are sessile. On the contrary, among the 8 main taxa that showed a
24
25 310 decreased abundance and distribution, a majority is sessile (5) and a minority is mobile (3).

28 311 Table 2. Summary of taxa richness and changes from 2015 to 2017
29

Number of taxa	ACA* [3.7°S]	PVE [4.2°S]	PBA [4.7°S]	YAC [5.1°S]	PAG [5.8°S]	PUE [7.5°S]	TAM [10.3°S]	PUC [12.5°S]	MIN [13.9°S]
In 2015 (N ₀)	24	26	14	25	16	18	25	20	21
In 2017 (N ₁)	9	26	25	22	23	22	22	15	25
appearing (N _a)	5	13	18	7	13	14	7	7	12
disappearing (N _d)	20	13	7	10	6	10	10	12	8
persisting	4	13	7	15	10	8	14	8	13
net change	-15	0	11	-3	7	4	-3	-5	4
turnover % **	75.8	50	64.1	36.2	48.7	60	36.2	54.3	43.5

42 312 * This site was not representative of the rocky intertidal in 2017

43 313 ** $100(N_a+N_d)/(N_0+N_1)$
44
45 314
46
47

48 315 3.2. Species richness and species turnover

49
50
51 316 The differences in the Chao2 richness estimator from 2015 to 2017 does not show any clear
52
53 317 geographical pattern. When considering all sites together, no significant difference was detected in
54
55
56 318 species richness between 2015 and 2017, neither for mobile, sessile taxa, or all taxa together
57
58 319 (Wilcoxon signed rank test, and t-test, $p>0.95$ in all cases). Thus, at regional scale, no significant
59
60
61
62
63
64
65

1
2
3 320 increase nor decrease in the taxonomic richness as estimated by the Chao2 index was detected four
4
5 321 months after the El Niño events.
6
7
8 322 Some substantial changes were site specific. A strong reduction of species richness is observed in
9
10 323 2017 in ACA[3.7°S], which can be explained by a significant increase of sand coverage (t-test,
11
12
13 324 $p < 0.05$) in this site and the subsequent reduction of the rocky intertidal (only two mobile species
14
15 325 were registered while 8.5 mobile species per site were registered in average). In other sites, rock
16
17
18 326 coverage did not vary among sampling sets (Wilcoxon signed ranks test, $p = 0.91$), and sand coverage
19
20 327 of the rocky shore areas was zero south of 5° S. This change in ACA[3.7°S] was possibly the result
21
22
23 328 of coastal geomorphological dynamics due to increased river discharge and sandbank movement
24
25 329 during the 2017 El Niño event (Rodríguez-Morata *et al.*, 2018).
26
27
28 330 The large decrease in species richness observed in the southern site PUL[12°S] is likely related to the
29
30
31 331 incomplete sampling in 2015 when only 8 out of 16 quadrats could be sampled because of logistics
32
33 332 constraints. This results in a large data dispersal in the Chao2 index for 2015. A significant increase
34
35
36 333 in species richness is observed in PAG[5.8°S], a site that lies in the biogeographic transition zone.
37
38 334 The number of taxa recorded in this site increased from 16 in 2015 to 23 in 2017 (Table 2). This net
39
40
41 335 increase is composed by a loss of 6 species (2 mobile and 4 sessile) and a gain of 13 species (7
42
43 336 mobile, 6 sessile). The largest net increase in the number of species is observed in PBA[4.7°S] with
44
45 337 11 additional species in 2017 (2 mobile, 9 sessile) compared to 2015. However, the small difference
46
47
48 338 in the Chao2 index values suggest this may mainly result from under-representation of the 2015
49
50 339 sample.
51
52
53 340 The turnover of taxa from 2015 to 2017 is relatively high (Table 2), from 36% taxa in TAM[10.3°S]
54
55
56 341 (17 taxa appearing or disappearing in the record) to 64% taxa in PBA[4.7°S] (25 taxa appearing or
57
58 342 disappearing in the record). One of the largest change in taxa is observed in the northern site
59
60 343 PVE[4.2°S], with 13 taxa that disappeared and 13 new species in the 2017 record compared to 2015.
61
62
63
64
65

1
2
3 344
4
5
6 345
7
8
9 346
10
11 347
12
13 348
14
15
16 349
17
18 350
19
20
21 351
22
23 352
24
25
26 353
27
28 354
29
30
31 355
32
33 356
34
35
36 357
37
38 358
39
40
41 359
42
43 360
44
45
46 361
47
48 362
49
50
51 363
52
53 364
54
55
56 365
57
58 366
59
60
61
62
63
64
65

3.3. Dissimilarities of rocky intertidal communities between 2015 and 2017

In the first nMDS ordination analysis, samples from 2017 are dissimilar to 2015 along axis 2, while both datasets are similarly distributed along axis 1 (Figure 6A). This latter result suggests that, in 2015 like in 2017, the communities are primarily structured by the same environmental factors. For instances, sites observed in 2017 after the El Niño events are similar along axis 1 as also observed for 2015. The axis 1, which explains 54% of the variability of the complete dataset, is clearly related to the latitudinal mean SST gradient (Figure 6B). The sites surveyed in 2017 are aligned along a similar relationship with mean annual SST as the 41 sites surveyed in 2015 (Figure 6B) confirming that the rocky intertidal communities are latitudinally structured, as already shown by Ibañez-Erquiaga et al. (2018), and that this latitudinal gradient persisted after the El Niño events.

The axis 2, which explains 33% of the variability, seems largely driven by the difference between 2015 and 2017. All the sites surveyed in 2017 show a positive shift along axis 2 since 2015 (arrows in figure 6A). Because a large proportion of taxa have been observed only once (~40%), we performed a nMDS analysis excluding singletons, which showed a similar pattern (Supplementary information). The separation of the 2015 and 2017 dataset along axis 2 is therefore not related to the occurrence of rare and potentially seasonal species, but rather to the changes in the distribution of important species described in section 3.1. The disappearance of *Austrolittorina araucana*, *Prisogaster niger*, and *Grateloupia filicina* in the 2017 samples together with the widespread apparition of *Mitrella baccata*, *Stramonita biserialis*, and *Phymactis clematis* played in particular a major role. As a consequence, the dissimilarity between the 2015 and 2017 surveys is likely due to environmental factors which may be related to El Niño or to seasonal variations since the 2015 observations were made between February and April while 2017 observations were made in October.

1
2
3 367 The similarity of the 9 sites surveyed in 2017 compared to the 41 sites surveyed in 2015 is observed
4
5 368 in a cluster analysis (Figure 7). Besides two 2105 sites separated because of anthropogenic impact
6
7
8 369 (ANC and BAR) and ACA[3.7°S] which was covered in sand in 2017, the sites are distributed in 4
9
10 370 groups, which, despite low bootstrap values, are biogeographically consistent. The northernmost site
11
12
13 371 of 2017 PVE[4.2°S] (pink branch), the Peruvian Panamic province (orange branches) in which
14
15 372 PBA[4.7°S] and PAG[5.8°S] are included in 2017, the transition zone (red) as defined in 2015, and
16
17
18 373 the Humboldt province in which 4 sites of 2017 are grouped together. All sites of the Humboldt
19
20 374 province in 2015 belong to the Humboldt province of 2017, except for the northernmost,
21
22 375 PAG[5.8°S], which appears in the Panamic province group in 2017. The cluster analysis indicates
23
24
25 376 that 2017 samples tend to group together within their respective ecological province, which confirms
26
27 377 that the change in rocky intertidal communities from 2015 to 2017 does not correspond to a
28
29
30 378 replacement of Humboldt communities by Panamic communities, but rather to the emergence of new
31
32 379 taxa assemblages. The outside position of PVE[4.2°S] in 2017 suggests the record of a dissimilar
33
34
35 380 Panamic community in northern Peru in 2017. This is supported by the fact that among the 13 new
36
37 381 taxa observed in PVE[4.2°S] in 2017, 8 have not been observed in any other site, and 2 were only
38
39 382 observed further north in ACA[3.7°S] in 2015.

41
42 383
43

44 45 384 **3.4. The latitudinal structure of rocky intertidal communities** 46 47

48 385 Whatever their cause, the differences between 2015 and 2017 evidence a strong seasonal to
49
50
51 386 interannual variability of rocky shore communities. The 2017 observations were pooled with the
52
53 387 2015 observations from the same sites and analyzed to test the robustness of the biogeographical
54
55
56 388 zonation found in rocky intertidal communities by Ibañez-Erquiaga et al. (2018) to this interannual
57
58 389 variability. The nMDS ordination analysis of the pooled dataset provided a pattern that is consistent
59
60
61 390 with the site latitudinal sequence (Figure 8A). The nMDS analysis showed a slight horseshoe effect,
62
63
64
65

1
2
3 391 which is common in ordination techniques due to the fact that the axes are forced to be uncorrelated,
4
5 392 but are not necessarily independent (Legendre and Gallagher, 2001). The first axis explained 84% of
6
7
8 393 the ordination and the second axis 1%.

9
10
11 394 We evaluated the relationship between the long-term persisting geographical structure of the rocky
12
13 395 intertidal communities with long-term SST statistics. The first axis was significantly and strongly
14
15 396 correlated with mean annual SST ($R=0.93$, $p=0.001$) (Figure 8B) and mean SST of July (winter)
16
17 397 ($R=0.89$, $p=0.001$). Statistically significant spatial autocorrelations ($p<0.05$) were observed between
18
19 398 these two variables and the first axis, however, in both cases GLS maintain significant correlations
20
21 399 ($p=0.0001$ for the mean annual SST and $p=0.004$ for the mean SST of July) with lower AIC values
22
23 400 (23.29 and 23.92, respectively) improving the explanatory power of the model (Supplementary
24
25 401 information). The correlation observed between the first axis and with mean SST of February
26
27 402 (summer) ($R=0.77$, $p=0.195$, $R_{P0.8}=0.79$, $\text{power}=0.87$) was not significant, suggesting that summer
28
29 403 temperatures are less determinant than winter temperatures in the biogeography of rocky intertidal
30
31 404 species. On the other hand, no correlation was observed between the ordination's first axis and long-
32
33 405 term ENSO-related variability ($R=0.10$, $p=0.82$, $R_{P0.8}=0.79$, $\text{power}=0.06$) (Figure 8C) nor with the
34
35 406 mean seasonal SST range ($R=0.06$, $p=0.872$, $R_{P0.8}=0.79$, $\text{power}=0.05$).

36
37
38 407 The cluster analysis of the pooled incidence dataset (Euclidian cluster, $R=0.93$) confirms that the
39
40 408 latitudinal organization of rocky intertidal communities found in the snapshot observation of 2015, is
41
42 409 maintained when the interannual variability is integrated (Figure 9). Locations were grouped into two
43
44 410 main branches: the northern branch, corresponding to warm conditions of the Panamic province
45
46 411 includes ACA[3.7°S] and PVE[4.2°S]. The southern branch is itself divided in two groups: the
47
48 412 transition zone, which includes three sites located to the north of the Illescas Peninsula, PBA[4.7°S],
49
50 413 YAC[5.1°S] and PAG[5.8°S], and the Humboldt province which includes the 4 remaining
51
52 414 southernmost sites. High bootstrap scores indicate a robust structure.

53
54
55
56
57
58
59
60
61
62
63
64
65

1
2
3 415
4
5
6 416
7
8
9 417
10
11
12 418
13
14 419
15
16
17 420
18
19 421
20
21 422
22
23
24 423
25
26 424
27
28
29 425
30
31 426
32
33
34 427
35
36 428
37
38
39 429
40
41 430
42
43 431
44
45
46 432
47
48 433
49
50
51 434
52
53 435
54
55
56 436
57
58 437
59
60 438
61
62
63
64
65

4. Discussion

4.1. Changes in taxonomic diversity

The effects of El Niño on intertidal communities depend on the intensity and magnitude of the event. Although, the coupled oceanographic-atmosphere variability is similar, the biological responses are not always predictable (Arntz *et al.* 2006). Some responses are similar among events, strong El Niño (1982-83 and 1997-98) increased the diversity of macrobenthos on hypoxic soft-bottoms due to the increase of oxygen concentration, and colonization by low latitude immigrant species in central Peru (Tarazona *et al.* 1988a,b). Also, neritic fish assemblages would add tropical species and cold-adapted fish would extend their distributional ranges down to central Chile (Sielfeld *et al.* 2010). In rocky shore communities the most important change documented is the mass mortality of kelp beds (Martínez *et al.* 2003) which could open rocky primary space in Peru and northern of Chile. This could trigger the colonization and recovery of communities via immigration and settlement of surviving species, but there is no available evidence on how this could affect diversity patterns. Our results indicate that, at the scale of the north-central Peruvian coast, the 2015-2016 and the 2017 El Niño events did not promote an overall change in the taxonomic richness of rocky intertidal communities. The disappearing of species between the two surveys was in average compensated by the occurrence of new species. We tested whether this could mask spatial contrasts related to the fact that the 2017 El Niño SST anomaly was not of equal amplitude along the latitudinal transect of our study. SST anomalies peaked everywhere during March 2017 (Figure 2), but were highest (5-6°C) along the central coast between 5 and 9°S (Figure 3F), and limited to 1-2°C in the northernmost and southernmost sites. No significant relationship is observed between the amplitude of the El Niño 2017 SST anomaly and the Chao2 estimator change, nor with the level of taxa turnover, which may be partly due to the low statistical power resulting from the limited number of sites. However, the

1
2
3 439 largest increase in Chao2 index was observed in PAG[5.8°S], the largest net increase in taxonomic
4
5 440 richness in PBA[4.7°S], and the largest turnover in PBA[4.7°S] and PUE[7.5°S]. All these sites
6
7
8 441 experienced El Niño SST anomalies larger than 5°C, supporting some level of impact of the 2015
9
10 442 and 2017 El Niño events on rocky intertidal diversity, especially in the transition zone.
11
12

13 443

14

15

16 444 **4.2. Changes in species distribution**

17

18

19 445 The warm anomaly associated to an El Niño event may be a stressor for some species and may
20
21 446 favour others, while some El Niño adapted species would show no response at all (e.g. Barahona *et*
22
23
24 447 *al.* 2019). Overall, it could be predicted that El Niño produces a southward shift of species, either by
25
26 448 inducing mortality in the northern limit of their distribution where conditions would exceed some
27
28
29 449 physiological or ecological threshold, or by favouring a migration towards higher latitudes (Riascos
30
31 450 *et al.*, 2009; Sotil *et al.*, 2008; Carstensen *et al.*, 2010). Here, we found that the average shift of
32
33
34 451 incidence median latitude is non-significant for mobile or sessile taxa (t-test). The large distribution
35
36 452 changes observed for some taxa were not all directed southward.
37
38

39 453 Based on presence/absence analysis a pattern among sites and years emerge. Mobile gastropods such
40
41 454 as *Fissurella* spp., *Mitrella baccata*, *Scurria* spp., *Stramonita biserialis*, and the sea anemone
42
43
44 455 *Phymactis clemactis* were present in most of the sites sampled in 2017 but almost absent in 2015.
45
46 456 These species are mobile and while they can inhabit exposed rocky surfaces, they can also move into
47
48
49 457 crevices and sheltered areas of the habitat. Thus, these species may undergo undetected during
50
51 458 sampling, but it is unlikely that this may have happened at multiple sites. The same reasoning applies
52
53
54 459 to those taxa present in 2015 but absent or strongly reduced in 2017: gastropods *Austrolittorina*
55
56 460 *araucana*, *Prisogaster niger*, *Siphonaria* spp., the anemone *Phymanthea pluvia*, but not for the
57
58
59 461 mytilid *Semimytilus algosus*, and algae *Grateloupia filicina*, *Gymnogongrus durvillei*, and
60
61 462 *Polysiphonia* spp.. *G. filicina* is considered an annual species, with plants showing higher
62
63
64
65

1
2
3 463 abundances and sizes during summer, and re-growing from the perennial attachment disc in spring
4
5 464 after overwintering (Irvine 1983). The absence of *G. filicina* during 2017 spring could be explained
6
7
8 465 by the fact that the perennial attachment disc is difficult to identify in the field or by the small size of
9
10 466 young plants growing from it. In contrast, *G. durvillei* is usually found all year in central and north-
11
12
13 467 central coast of Peru (Hidalgo et al. 2008; Li-Alfaro and Zafra-Trelles 2012; Pisfil-Farro 2014;
14
15 468 Rojas-Paredes 2014). Its absence in multiple sites during spring 2017 could not be attributed to
16
17
18 469 seasonality and is likely linked to El Niño events. *S. algosus* (Tarazona et al. 1985) and other
19
20 470 mytilids (e.g., Gamarra and Cornejo 2002; Avendaño and Cantillanez 2011) have been reported to
21
22 471 experience mortality and recruitment failure during and after strong El Niño events.
23
24
25 472 The ecology and seasonality of most marine species from Peru remains unknown. In the absence of
26
27
28 473 long-term control observations, we cannot clearly attribute the observed changes in distribution and
29
30 474 abundance to seasonal processes or to El Niño perturbations (Paine, 1986). Sessile taxa should,
31
32
33 475 however, exhibit less seasonal variation in the presence/absence data and may thus reflect more
34
35 476 closely direct or indirect El Niño impacts. Among widespread sessile species, 2 were completely
36
37
38 477 absent in 2017 (*G. filicina*, *Polysiphonia spp.*) and 3 were strongly reduced (*G. durvillei*, *P. pluvia*,
39
40 478 and *S. algosus*) and all shifted south, which is consistent with a SST-related stress. Some sites reveal
41
42 479 some interesting changes: the fact that PAG[5.8°S] taxon assemblage belonged to the Humboldt
43
44
45 480 province in 2015 and to the transition branch after the El Niño events in 2017 (Figure 7) suggests that
46
47 481 the new rocky intertidal community in this site is at least partly due to southward species migration
48
49
50 482 facilitated by El Niño conditions from 2015 to 2017. The occurrence of 8 new Panamic species in
51
52 483 PVE[4.2°S] in 2017, which places this northernmost assemblage outside the cluster analysis (Figure
53
54
55 484 7), also supports a southward migration of species consistent with the expected impact of El Niño
56
57 485 events.
58
59
60
61
62
63
64
65

1
2
3 486 Some taxa, on the other hand, do not fit in this scenario. The three sessile taxa that widely spread
4
5 487 from 2015 to 2017 (*Corallina officinalis*, encrusting brown algae, *Phymactis clematis*) are not warm
6
7
8 488 water taxa but ubiquitous taxa, that expanded in both Panamic and Humboldt provinces. A few
9
10 489 species also show an interesting northward expansion (brown algae *Colpomena tuberculata*,
11
12
13 490 *Colpomena sinuosa*). The expansion of those species was therefore not caused by favourable physical
14
15 491 conditions during El Niño events, but was more likely an indirect consequence of those events
16
17
18 492 through a modified ecological network.
19

20 493
21

23 494 **4.3. El Niño impacts on community structure**

24
25
26 495 Changes in community structures between 2015 and 2017 are evidenced in the nMDS (Figure 6) and
27
28
29 496 the cluster analysis (Figure 7). These changes are linked to large changes in the latitudinal
30
31 497 distribution of a few widespread species, likely caused, at least for some of them, by El Niño regional
32
33
34 498 environmental anomalies occurred in 2015-2016 and 2017. Quantifying how much of the community
35
36 499 change can be attributed to El Niño and how much to seasonal variations will require additional
37
38
39 500 surveys in those sites.
40

41 501 The change in the communities from 2015 to 2017 was not characterized by a shift along a
42
43
44 502 temperature-related axis (axis 1 of nMDS analysis, Figure 6) as one could expect from El Niño
45
46 503 impacts. The 2017 communities are thus not simply the result of the southward migration of species
47
48
49 504 and the replacement of "temperate" taxa by "Panamic" taxa. This process, which has been reported
50
51 505 for earlier extreme El Niño events (Tarazona et al. 1988a,b; Arntz et al. 2006) was only secondary
52
53
54 506 here, possibly because the amplitude and duration of the temperature anomaly was not as large than
55
56 507 in those extreme events. The primary process responsible for the 2015 to 2017 community change
57
58
59 508 might thus be ecological.
60
61
62
63
64
65

1
2
3 509 Since some of the taxa impacted here are major component of the rocky intertidal communities, we
4
5 510 can speculate that their local disappearing or expansion produced a secondary positive or negative
6
7
8 511 impact on other taxa that had not been directly affected by the physical or chemical anomalies
9
10 512 associated to the El Niño events. In this view, the physico-chemical conditions of El Niño may have
11
12
13 513 only been the trigger of a chain of impacts across the ecological network of Peruvian rocky shores. A
14
15 514 detailed study of the ecological interactions between the most impacted species would be needed to
16
17
18 515 test this hypothesis.

19
20
21 516

22 23 517 **4.4. Robustness of the biogeographic zonation**

24
25
26 518 Merging the 2015 and 2017 dataset integrates part of the seasonal and interannual variability which
27
28
29 519 therefore provides us with a dataset that is more representative of the long-term biogeographical
30
31 520 features. The nMDS (Figure 8) and the Euclidian cluster (Figure 9) analyses on the merged dataset
32
33
34 521 showed a latitudinally coherent pattern of the rocky shore communities, coinciding with the
35
36 522 biogeographic zonation proposed by Ibañez-Erquiaga *et al.* (2018) based on a snapshot picture of the
37
38
39 523 rocky shore communities before the El Niño event. The coastal sites are divided in 3 groups
40
41 524 belonging to the Panamic province in the north, the Humboldt Province in the central coast, and a
42
43 525 transition zone that shares more similarity with the Humboldt province than with the Panamic
44
45
46 526 province (Figure 9). The zonation obtained with the joint dataset suggests that the exposition to the
47
48 527 2015-16 and 2017 El Niño events and the change in communities described above did not alter the
49
50
51 528 biogeographical structure of rocky intertidal species along the Peruvian coast. The dominant axis that
52
53 529 structures the sites in the nMDS analysis is strongly correlated with mean surface temperature
54
55
56 530 (Figure 8B), especially winter temperature. This is consistent with the fact that the community
57
58 531 change from 2015 to 2017 is described by nMDS axis 2, which is independent from axis 1 related to
59
60
61 532 mean SST (Figure 6).

62
63
64
65

1
2
3 533 No correlation is observed with long-term ENSO variance (Figure 8C). This shows that interannual
4
5 534 temperature anomalies, although very high in Peru for the influence of ENSO, do not play a primary
6
7
8 535 role in the latitudinal structure of rocky intertidal communities in the northern and central coast of
9
10 536 Peru. Additional environmental factors besides SST, wave impact, water oxygen content, nutrient
11
12
13 537 concentration and air temperature, may be determinant in the biogeographical distribution of the
14
15 538 intertidal rocky communities and require further studies. Broitman *et al.* (2001) showed that more
16
17
18 539 than mean SST and latitude, the influence of coastal upwelling cells was the driving force in the
19
20 540 geographic patterns in the rocky intertidal of Central Chile. Another comprehensive study in Chile
21
22 541 (assessing about 24° of latitude between 18°S and 42°S) showed a mid-latitudinal peak (at 30-32°S)
23
24
25 542 in species diversity (Rivadeneira *et al.*, 2002) that could be due to a combination of regional
26
27 543 environmental conditions and local ecological interactions. In the same sense, Ibañez-Erquiaga *et al.*
28
29
30 544 (2018) found phosphate concentrations to be one of the main potential drivers of biogeographic
31
32 545 patterns at the intertidal communities at the Peruvian coast. Further work, increased sampling
33
34
35 546 resolution, analysis of additional variables, and long-term ecological records are needed in Peru to
36
37 547 describe more precisely the role of upwelling cells and ecological relationships in the rocky intertidal
38
39
40 548 communities and disentangle these variables from the SST which is strongly linked to the coastal
41
42 549 upwelling in this region.

43 44 45 550 46 47 48 551 **5. Conclusions**

49
50
51 552 We have presented the first insights into the response of the rocky intertidal community to two
52
53 553 successive El Niño event in Peru (2015-16 and 2017) by analyzing the taxonomic diversity of
54
55
56 554 macrobenthic species, their geographic distribution, and the latitudinal structure of communities
57
58 555 observed in austral fall 2015 after 17 years of stable La Niña conditions and in austral spring 2017,
59
60
61 556 four months after the end of the 2017 coastal El Niño event. The 2017 El Niño produced during
62
63
64
65

1
2
3 557 about three months a strong SST anomaly in the central and northern coast of Peru (Echevin et al.,
4
5 558 2018) that reached 6°C at its maximum and triggered strong rainfalls (Rodríguez-Morata *et al.* 2018).
6
7
8 559 We find that four months after this violent environmental disturbance, the taxonomic richness has not
9
10 560 significantly changed at the regional scale, but an important turnover of species was observed
11
12
13 561 everywhere, and especially in the transition zone, where the highest SST anomalies occurred. A
14
15 562 southward migration of taxa, resulting from the southward shift of SST pattern during El Niño events
16
17
18 563 in this region, has apparently occurred in some sites of northern Peru, especially in PVE[4.2°S]
19
20 564 where eight Panamic species appeared. However, this mechanism did not trigger a strong latitudinal
21
22 565 change on the structure of the communities. While the rocky shore communities are clearly structured
23
24
25 566 along a latitudinal SST gradient, the change in species assemblages observed in 2017 occurred in a
26
27 567 direction independent from this SST gradient. The change in species assemblages was mainly driven
28
29
30 568 by the large distribution reduction of some important widespread species (*Austrolittorina araucana*,
31
32 569 *Prisogaster niger*, *Siphonaria* spp., *Grateloupia filicina*, *Gymnogongrus durvillei*, *Phymanthea*
33
34
35 570 *pluvia*, *Semimytilus algosus*) and the spread of some other species (*Fissurella* spp., *Mitrella baccata*,
36
37 571 *Scurria* spp., *Stramonita biserialis*, *Corallina officinalis*, *Phymactis clematis*). In the absence of long-
38
39 572 term record of the rocky intertidal communities in Peru, the change observed from 2015 to 2017
40
41
42 573 cannot be simply attributed to seasonal variations or to the El Niño events. However, since some of
43
44 574 these important species are clearly not seasonal, we must conclude that at least part of these changes
45
46
47 575 was caused by large scale regional environmental perturbations associated to the 2015-16 and 2017
48
49 576 El Niño events. The primary environmental impact on some ecologically key species likely triggered
50
51
52 577 a chain of secondary impacts through ecological relationships which lead to a complex change in
53
54 578 rocky shore communities. Further studies are needed to better characterize the seasonal and
55
56
57 579 interannual variability of the rocky intertidal communities and their drivers. When this interannual
58
59 580 variability is integrated, the 9 study sites show a very robust structure determined by the latitudinal
60
61 581 SST gradient along the Peruvian coast.
62
63
64
65

1
2
3 582
4
5
6 583
7
8
9 584
10
11 585
12
13
14 586
15
16 587
17
18
19 588
20
21 589
22
23
24 590
25
26
27 591
28
29
30 592
31
32 593
33
34
35 594
36
37 595
38
39
40 596
41
42
43 597
44
45
46 598
47
48 599
49
50
51 600
52
53 601
54
55
56 602
57
58
59 603
60
61
62
63
64
65

Acknowledgments

Fieldwork permits in natural protected areas were provided by the National Authority of Natural Protected Areas SERNANP. We are very thankful to Diego Cuba, Leonardo Hostos, and Julisa Bermudez for their support in the field work and to Alexa Narciso, Katherine Campos, Julisa Bermudez, Leonardo Hostos and Iván Vásquez for their lab support. We thank three anonymous reviewers that help us to improve an early version of this manuscript.

Author Contributions

JV and MC conceived the project idea. BI, JV and MPH carried out the field and laboratory work. BI, LW, JV, MPH and AI carried out the invertebrate identification. JAP, JV, BI and LW carried out the algae identification. JV, MC, ASP, BI, DO performed the data analysis. RSG, DO, JC, ASP aided in interpreting the results and worked on the manuscript. All authors discussed the results, provided critical feedback and contributed to the final manuscript.

Funding

This study was supported by the FONDECYT (Peru) academic research grant to the Master's Program on Marine Sciences at the Universidad Peruana Cayetano Heredia (N° 014-2013-FONDECYT), and by CONCYTEC (Peru) research grants MAGNET (N° 007-2017-FONDECYT) and "incorporación de investigadores" (N° E038-2019-02-FONDECYT-BM).

Conflict of Interest

1
2
3
4
5
6
7
8
9
10
11
12
13
14
15
16
17
18
19
20
21
22
23
24
25
26
27
28
29
30
31
32
33
34
35
36
37
38
39
40
41
42
43
44
45
46
47
48
49
50
51
52
53
54
55
56
57
58
59
60
61
62
63
64
65

604 The authors declare that the research was conducted in the absence of any commercial or financial
605 relationships that could be construed as a potential conflict of interest.

606
References

608 Aguilera, M. A., Valdivia, N., Broitman, B. R. (2013). Spatial niche differentiation and coexistence
609 at the edge: co-occurrence distribution patterns in *Scurria* limpets. *Marine Ecology Progress*
610 *Series*, 483, 185-198.

611 Arntz, W. E. (1986). The two faces of El Niño 1982-83. *Meeresforschung*. 31(I): 1-46.

612 Arntz, W.E., Brey, T., Tarazona, J., Robles, A. (1987). Changes in the structure of a shallow sandy-
613 beach community in Peru during an El-Niño event. *S Afr J Marine Sci.* 5, 645–658.

614 Arntz, W.E., Valdivia, E., Zeballos, J. (1988). Impact of El Niño 1982–83 on the commercially
615 exploited invertebrates (mariscos) of the Peruvian shore. *Meeresforschung*. 32, 3–22.

616 Arntz, W.E., Gallardo, V. A., Gutiérrez, D., Isla, E., Levin, L. A., et al. (2006). El Niño and similar
617 perturbation effects on the benthos of the Humboldt, California, and Benguela Current upwelling
618 ecosystems. *Advances in Geosciences. Enrgy Proced.* 6, 243-265.

619 Avendaño, M., Cantillanez, M. (2011). Reestablishment of *Choromytilus chorus* (Molina, 1782)
620 (Bivalvia: Mytilidae) in northern of Chile. *Lat. Am. J. Aquat. Res.* 39(2), 390-396.

621 Barahona, S.P., Vélez-Zuazo, X., Santa-Maria, M., & Pacheco, A.S. (2019). Phylogeography of the
622 rocky intertidal periwinkle *Echinolittorina paytensis* through a biogeographic transition zone in
623 the Southeastern Pacific. *Mar. Ecol.* 00:e12556. <https://doi.org/10.1111/maec.12556>

624 Barber, R.T., Chavez, F.P. (1983). Biological consequences of El Niño. *Science*. 222, 1203-1210.

625 Bivand, RS, Pebesma, E, Gomez-Rubio, V (2013). *Applied spatial data analysis with R*, Second
626 edition. Springer, NY. <http://www.asdar-book.org/>.

1
2
3 627 Blanchette, C.A., Melissa Miner, C., Raimondi, P.T., Lohse, D., Heady, K.E.K., Broitman, B.R.
4
5 628 (2008). Biogeographical patterns of rocky intertidal communities along the Pacific coast of
6
7
8 629 North America. *Journal of Biogeography* 35, 1593–1607. <https://doi.org/10.1111/j.1365->
9
10 630 2699.2008.01913.x
11
12
13 631 Broitman, B.R., Navarrete, S.A., Smith, F., Gaines, S.D., (2001). Geographic variation of
14
15 632 southeastern Pacific intertidal communities. *Mar Ecol Prog Ser.* 224, 21-34.
16
17
18 633 Broitman, B.R., Véliz, F., Manzur, T., Wieters, E., Finke, R., Fornes, P., Valdivia, N., Navarrete,
19
20 634 S.A. (2011). Geographic variation in diversity of wave exposed rocky intertidal communities
21
22 635 along central Chile. *Rev Chil Hist Nat.* 224, 21-34.
23
24
25 636 Castilla, J.C., Camus, P.A. (1992). The Humboldt–El Niño scenario — coastal benthic resources and
26
27 637 anthropogenic influences, with particular reference to the 1982/83 ENSO. *S Afr J Marine Sci.*
28
29
30 638 12, 703–712.
31
32 639 Camus, P. (2008). Understanding biological impacts of ENSO on the eastern Pacific: an evolving
33
34
35 640 scenario. *Int J Environ Heal R.* 2(1): 5-18.
36
37 641 Cane, M. A. (1983). Oceanographic events during El Niño. *Science.* 222, 1189-1195.
38
39
40 642 Carré, M., Sachs, J. P., Schauer, A. J., Rodríguez, W. E., Ramos, F. C. (2013). Reconstructing El
41
42 643 Niño-Southern Oscillation activity and ocean temperature seasonality from short-lived marine
43
44 644 mollusk shells from Peru. *Palaeogeography, Palaeoclimatology, Palaeoecology,* 371, 45-53.
45
46
47 645 Carstensen, D., Riascos, J. M., Heilmayer, O., Arntz, W. E., Laudien, J. (2010). Recurrent,
48
49 646 thermally-induced shifts in species distribution range in the Humboldt current upwelling system.
50
51
52 647 *Marine Environmental Research,* 70, 293- 99. Doi: [10.1016/j.marenvres.2010.06.001](https://doi.org/10.1016/j.marenvres.2010.06.001)
53
54 648 Chao, A., Colwell, R.K., Lin, C.-W., Gotelli, N.J. (2009). Sufficient sampling for asymptotic
55
56 649 minimum species richness estimators. *Ecology* 90, 1125–1133. <https://doi.org/10.1890/07->
57
58
59 650 [2147.1](https://doi.org/10.1890/07-2147.1)
60
61
62
63
64
65

- 1
2
3 651 Chao, A., Ma, K. H., Hsieh, T. C., Chiu, C.H. (2016). SpadeR: Species-Richness Prediction and
4
5 652 Diversity Estimation with R. R package version 0.1.1. [https://CRAN.R-](https://CRAN.R-project.org/package=SpadeR)
6
7
8 653 [project.org/package=SpadeR](https://CRAN.R-project.org/package=SpadeR)
9
- 10 654 Diniz- Filho, J. A., Bini, L. M., Hawkins, B. A. (2003). Spatial autocorrelation and red herrings in
11
12 655 geographical ecology. *Global Ecology and Biogeography*, 12(1), 53-64.
13
14
- 15 656 Echevin, V., Colas, F., Espinoza-Morriberon, D., Vasquez, L., Anculle, T., Gutierrez, D., 2018.
16
17 657 Forcings and Evolution of the 2017 Coastal El Niño Off Northern Peru and Ecuador. *Frontiers in*
18
19 658 *Marine Science* 5, 367. <https://doi.org/10.3389/fmars.2018.00367>
20
21
- 22 659 Espino, M. (1999) El Niño 1997-98: Su efecto sobre el ambiente y los recursos pesqueros en el Perú.
23
24 660 *Rev Peru Biol. Vol. Extraordinario: 97-109*
25
26
- 27 661 Faul, F., Erdfelder, E., Buchner, A., Lang, A.-G. (2009). Statistical power analyses using G*Power
28
29 662 3.1: Tests for correlation and regression analyses. *Behavior Research Methods*, 41, 1149-1160.
30
31
- 32 663 Gamarra, A., Cornejo, O. (2002). Study of the mussel *Aulacomya ater* Molina, 1782 (Bivalvia:
33
34 664 Mytilidae) near Santa Rosa Island, Independence Bay, during El Niño phenomenon 1997-98.
35
36 665 *Investig. Mar.* 30(Supl. 1) <http://dx.doi.org/10.4067/S0717-71782002030100045>
37
38
- 39 666 Garreaud, R. D. (2018), A plausible atmospheric trigger for the 2017 coastal El Niño, *International*
40
41 667 *Journal of Climatology*, 38, e1296-e1302.
42
43
- 44 668 Glynn, P.W. (1988). El Niño Southern Oscillation 1982–1983 — nearshore population, community,
45
46 669 and ecosystem responses. *Ann Rev Ecol S.* 19, 309–345.
47
48
- 49 670 Gotelli, N.J., Colwell, R.K. (2001). Quantifying biodiversity: procedures and pitfalls in the
50
51 671 measurement and comparison of species diversity. *Ecol Lett.* 4, 379–391.
52
53
- 54 672 Hammer, O., Harper, D.A.T. and Ryan, P.D. (2000). PAST; paleontological statistics software
55
56 673 package for education and data analysis. *Palaeontologia Electronica*, 4(1): 9.
57
58
- 59 674 Hidalgo, F.J., Firstater, F.N., Fanjul, E., Cielo Bazterrica, M., Lomovasky, B.J., Tarazona, J.,
60
61 675 Iribarne, O.O. (2008) Grazing effects of the periwinkle *Echinolittorina peruviana* at a central
62
63
64
65

1
2
3 676 Peruvian high rocky intertidal. *Helgol. Mar. Res.* 62 (suppl 1):S73–S83. doi:10.1007/s10152-
4
5 677 007-0086-3
6
7
8 678 Huang, B., L'Heureux, M., Hu, Z.-Z., Zhang, H.-M. (2016). Ranking the strongest ENSO events
9
10 679 while incorporating SST uncertainty. *Geophysical Research Letters.* 43, 9165-9172.
11
12
13 680 Ibañez-Erquiaga, B., Pacheco A.S., Rivadeneira, M.M., Tejada, C.L. (2018) Biogeographical
14
15 681 zonation of rocky intertidal communities along the coast of Peru (3.5–13.5° S Southeast Pacific).
16
17 682 PLoS ONE 13(11): e0208244.
18
19
20 683 Irvine, L. M. (1983). *Seaweeds of the British Isles. Vol 1: Rhodophyta. Part 2A Cryptonemiales*
21
22 684 (sensu stricto) *Palmariales, Rhodymeniales.* British Museum, London.
23
24
25 685 JPL MUR MEaSURES Project. 2015. GHRSSST Level 4 MUR Global Foundation Sea Surface
26
27 686 Temperature Analysis (v4.1). Ver. 4.1. PO.DAAC, CA, USA. <https://doi.org/10.5067/GHGMR->
28
29 687 [4FJ04](https://doi.org/10.5067/GHGMR-4FJ04).
30
31
32 688 Legendre, P., Gallagher, E.D. (2001). Ecologically meaningful transformations for ordination of
33
34 689 species data. *Oecologia.* 129, 271-280. doi:10.1007/s004420100716.
35
36
37 690 Li-Alfaro, G., Zafra-Trelles, A. (2012). Composición, abundancia y diversidad de macroalgas en el
38
39 691 litoral de puerto Malabrigo, La Libertad - Perú 2009. *Sciéndo* 15, 33-42.
40
41
42 692 Martínez, A., Cárdenas, L., & Pinto, R. (2003) Recovery and genetic diversity of the intertidal kelp
43
44 693 *Lessonia nigrescens* (Phaeophyceae) 20 years after El Niño 1982/83. *J. Phycol.* 39(3), 504-508.
45
46
47 694 Oksanen, J., Blanchet, F.G., Kindt, R., Legendre, R.G., O'Hara, B., Simpson, G.L., Solymos, P.,
48
49 695 Stevens, H.H. and Wagner, H. (2010). *Vegan: Community Ecology Package*, pp. R package
50
51 696 version 1.17-4, <http://CRAN.R-project.org/package=vegan>.
52
53
54 697 Paine, R. T. (1986). Benthic community-water column coupling during 1982-1983 El Niño. Are
55
56 698 community changes at high latitudes attributable to cause or coincidence? *Limnol. Oceanogr.*
57
58 699 31(2): 351-360.
59
60
61
62
63
64
65

1
2
3 700 Paredes, C. (1974). El modelo de zonación en la orilla rocosa del departamento de Lima. *Rev Peru*
4
5 701 *Biol*, 1, 168-191.
6
7
8 702 Paredes, C., Tarazona, J., Canahuire, E., Romero, L., Cornejo, O., Cardoso, F. (1998). Presence of
9
10 703 tropical mollusks from the Panamanian province in the central coast of Peru and relation with the
11
12
13 704 events "El Niño". *Rev Peru Biol*. 5(2): 123-128.
14
15 705 Peterman, R. M. (1990). Statistical power analysis can improve fisheries research and management.
16
17 706 *Canadian Journal of Fisheries and Aquatic Sciences*, 47(1), 2-15.
18
19
20 707 Pinheiro J, Bates D, DebRoy S, Sarkar D, R Core Team (2018). nlme: Linear and Nonlinear Mixed
21
22 708 Effects Models_. R package version 3.1-137, <https://CRAN.R-project.org/package=nlme>
23
24
25 709 Pisfil-Farro, J.C. (2014). Distribución de las macroalgas y su potencialidad en la bahía de Tortugas
26
27 710 (Casma, Perú) entre Noviembre 2011 y Febrero 2012. Thesis, Universidad Nacional del Santa,
28
29
30 711 Perú. Available on-line:
31
32 712 <http://200.37.61.90/bitstream/handle/UNS/2755/27216.pdf?sequence=1&isAllowed=y>
33
34
35 713 R-Core Team, 2013. R: A language and environment for statistical computing, R Foundation for
36
37 714 Statistical Computing. URL <http://www.R-project.org/>, Vienna, Austria.
38
39
40 715 Riascos, J. M., Carstensen, D., Laudien, J., Arntz, W. E., Oliva, M. E., Güntner, A., & Heilmayer, O.
41
42 716 (2009). Thriving and declining: climate variability shaping life-history and population
43
44 717 persistence of *Mesodesma donacium* in the Humboldt Upwelling System. *Marine Ecology*
45
46 718 *Progress Series*, 385, 151-163. <https://doi.org/10.3354/meps08042>
47
48
49 719 Rivadeneira, M., Fernández, M., Navarrete S. (2002). Latitudinal trends of species diversity in rocky
50
51
52 720 intertidal herbivore assemblages: spatial scale and the relationship between local and regional
53
54 721 species diversity. *Mar Ecol Prog Ser*. 245: 123-131.
55
56
57 722 Rivadeneira, M., Fernandez, M. (2005). Shifts in southern endpoints of distribution in rocky
58
59 723 intertidal species along the south-eastern Pacific coast. *J Biogeogr*. 32, 203-209.
60
61
62
63
64
65

- 1
2
3 724 Rodríguez-Morata, C., Díaz, H.F., Ballesteros-Canovas, J.A., Rohrer, M., Stoffel, M. (2018) The
4
5 725 anomalous 2017 coastal El Niño event in Peru. *Climate Dynamics*. doi: 10.1007/s00382-018-
6
7
8 726 4466-y.
9
- 10 727 Rojas-Paredes, N.L. (2014). Variación del macrobentos en el intermareal rocoso de Puerto Salaverry,
11
12 728 Huanchaco y Puerto Malabrigo, Región la Libertad durante Mayo-Julio del 2014. Unpublished
13
14
15 729 Thesis, Universidad Nacional de Trujillo, Perú. <http://dspace.unitru.edu.pe/>
16
- 17 730 Sielfeld, W., Laudien, J., Vargas, M., & Villegas, M. (2010). El Niño induced changes of the coastal
18
19
20 731 fish fauna off northern Chile and implication for ichthyography. *Rev. Mar. Biol. Oceano*. 45(S1),
21
22 732 705-722.
23
24
- 25 733 Sotil, G., Tarazona, J., Alvis, R., Francia, J. C., & Shiga, B. (2008). Comparative evaluation of the
26
27 734 DNA damage response in two Peruvian marine bivalves exposed to changes in temperature.
28
29
30 735 *Helgoland Marine Research*, 62(1), 101-105. <https://doi.org/10.1007/s10152-007-0100-9>
31
- 32 736 Tarazona, J., Salzwedel, H., Arntz, W.E. (1988a). Oscillations of macrobenthos in shallow waters of
33
34
35 737 the Peruvian central coast induced by El Niño 1982–1983. *J Mar Res*. 46, 593–611.
36
- 37 738 Tarazona, J., Salzwedel, H. and Arntz, W. (1988b) Positive effects of “El Niño” on macrozoobenthos
38
39 739 inhabiting hypoxic areas of the Peruvian upwelling. *Oecologia*. 76, 184–190.
40
41
- 42 740 Tarazona, J., Gutiérrez, D., Paredes, C., Indacochea, A. (2003). Overview and challenges of marine
43
44 741 biodiversity research in Peru. *Gayana*. 67, 206–231.
45
46
- 47 742 Tarazona, J., Paredes, C., Romero, L., Blaskovich, V., Guzman, S., & Sanchez, S. (1985).
48
49 743 Características de la vida planctónica y colonización de los organismos bentónicos epilíticos
50
51 744 durante el fenómeno El Niño. *Boletín Instituto del Mar del Perú*, Volumen Extraordinario 41-49.
52
53
- 54 745 Vazquez, J., Perry, K., Kilpatrick, K. (1998). NOAA/NASA AVHRR Oceans Pathfinder sea surface
55
56 746 temperature data set user's reference manual. Jet Propulsion Laboratory Tech Rep. D-14070.
57
58
- 59 747 Wang, C., Fiedler, P.C. (2006) ENSO variability and the eastern tropical Pacific: A review. *Prog*
60
61 748 *Oceanogr*. 69, 239-266.
62
63
64
65

1
2
3
4
5
6
7
8
9
10
11
12
13
14
15
16
17
18
19
20
21
22
23
24
25
26
27
28
29
30
31
32
33
34
35
36
37
38
39
40
41
42
43
44
45
46
47
48
49
50
51
52
53
54
55
56
57
58
59
60
61
62
63
64
65

749 Wyrtki, K. (1975). El Niño—The Dynamic Response of the Equatorial Pacific Ocean to Atmospheric
750 Forcing. *J Phys Oceanogr.* 5, 572-584.

FIGURE CAPTIONS

Figure 1. Map of the study area across the Peruvian Pacific coast. Black triangles show sampling locations with name, acronym and latitude. Brackets show the two biogeographic provinces.

Figure 2. SST anomalies (SSTa) from June 2002 to April 2018 for the 9 study sites, estimated from the Multi-scale Ultra-high Resolution (MUR) SST Analysis fv04.1. Note the remarkable spatial coherence of SST anomalies along the Peruvian coast. The two El Niño events of 2015/16 and 2017 are represented by the grey shaded bands. Black arrows indicate time intervals of the two sampling campaigns.

Figure 3. SST values off Peru from the Multi-scale Ultra-high Resolution (MUR) SST Analysis fv04.1. Gridded values are represented as shades in the left panels, while the values along the coastline are represented versus the latitude in the right panels. (A) mean annual SST, (B) mean seasonal SST range (shown in black and white, as it does not represent warm and cold waters), (C) mean SST for July (austral winter), (D) mean SST for February (austral summer), (E) SST anomaly variance, (F) SST anomaly of March 2017 (EN event). The 9 circles along the coastline represent sampling locations.

Figure 4. Rarefaction curves for the 9 sampling locations in 2015 (circles) and 2017 (triangles).

1
2
3
4
5
6
7
8
9
10
11
12
13
14
15
16
17
18
19
20
21
22
23
24
25
26
27
28
29
30
31
32
33
34
35
36
37
38
39
40
41
42
43
44
45
46
47
48
49
50
51
52
53
54
55
56
57
58
59
60
61
62
63
64
65

Figure 5. Species richness estimated by the Chao2 index in nine study sites for 2015 (blue circles) and 2017 (gray triangles).

Figure 6. (A) nMDS plot showing the pattern of dissimilarity in community structures using incidence data of the 2015 survey (Ibañez et al. 2018) (black dots, site latitude indicated as gray numbers) and the 2017 survey (blue dots, with site label). Dotted arrows show the change from 2015 to 2017 in the nine study sites. (B) Linear regression (red line) between nMDS scores (Axis 1) and sites' mean annual temperature. (see location codes in Table 1). The correlation coefficient and the p-values are indicated in red.

Figure 7. Sorensen-Dice Cluster including the 41 sites surveyed in 2015 (Ibañez-Erquiaga et al., 2018) (black labels) and the nine sites surveyed in 2017 (blue labels) using incidence data of both mobile and sessile taxa. Colors highlight the main clusters: Panamic province (orange), PVE site of 2017 (pink), the transition zone (red), and the Humboldt province (blue). Bootstrap values are indicated at each node.

Figure 8. (A) nMDS plot showing the pattern of dissimilarity in community structures of nine localities using 2015 and 2017 combined datasets. Correlation analysis between first Coordinate of nMDS graph with (B) mean annual SST and (C) ENSO-related SST variability.

Figure 9. Cluster (based on Sorensen-Dice index, $R=0.93$, number of bootstrap replicates: 10000) of the 9 sampling locations combining 2015 and 2017 incidence data of both sessile and mobile species. Bootstrap values are indicated at each node.

FIGURE 1

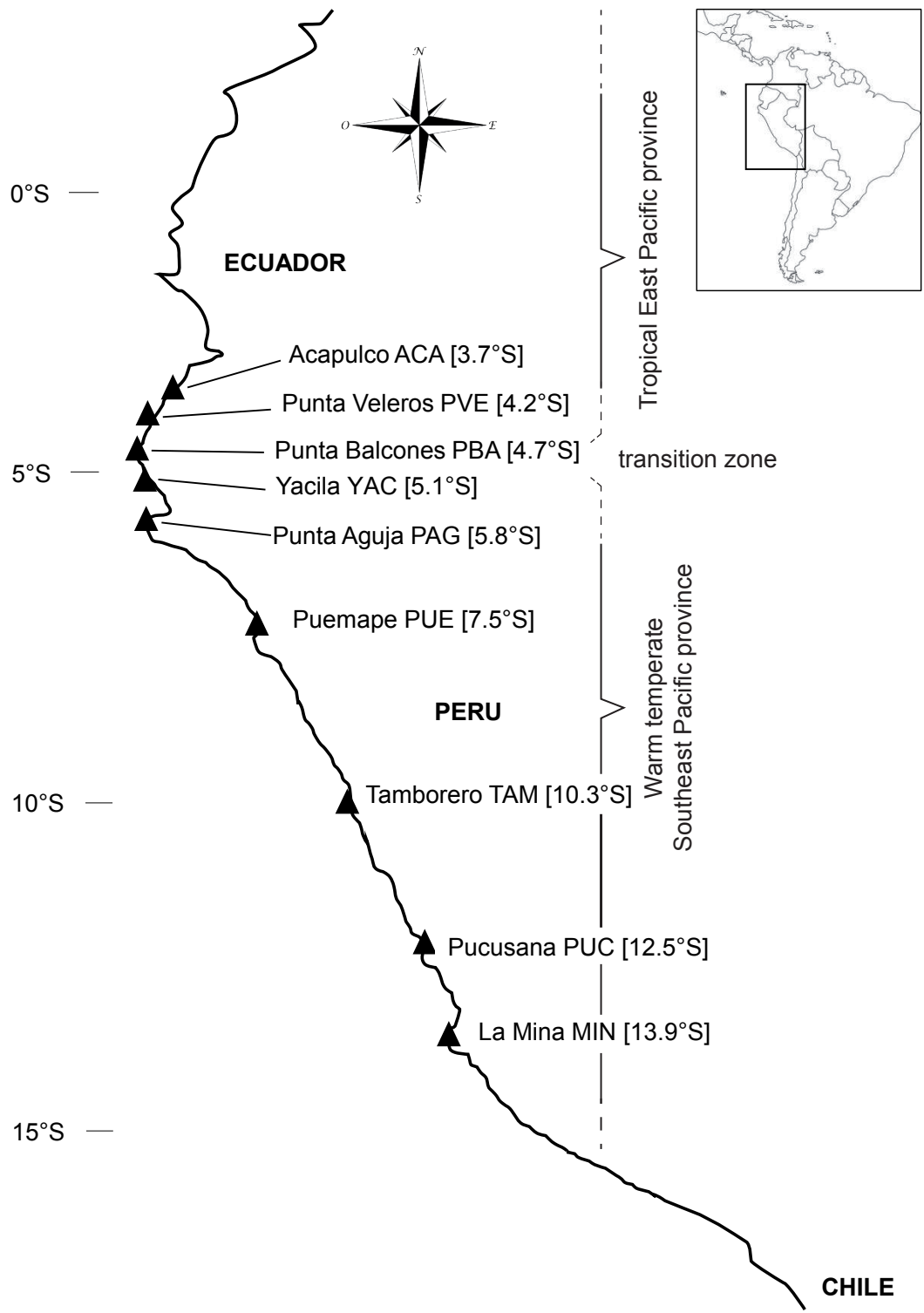


Figure 2

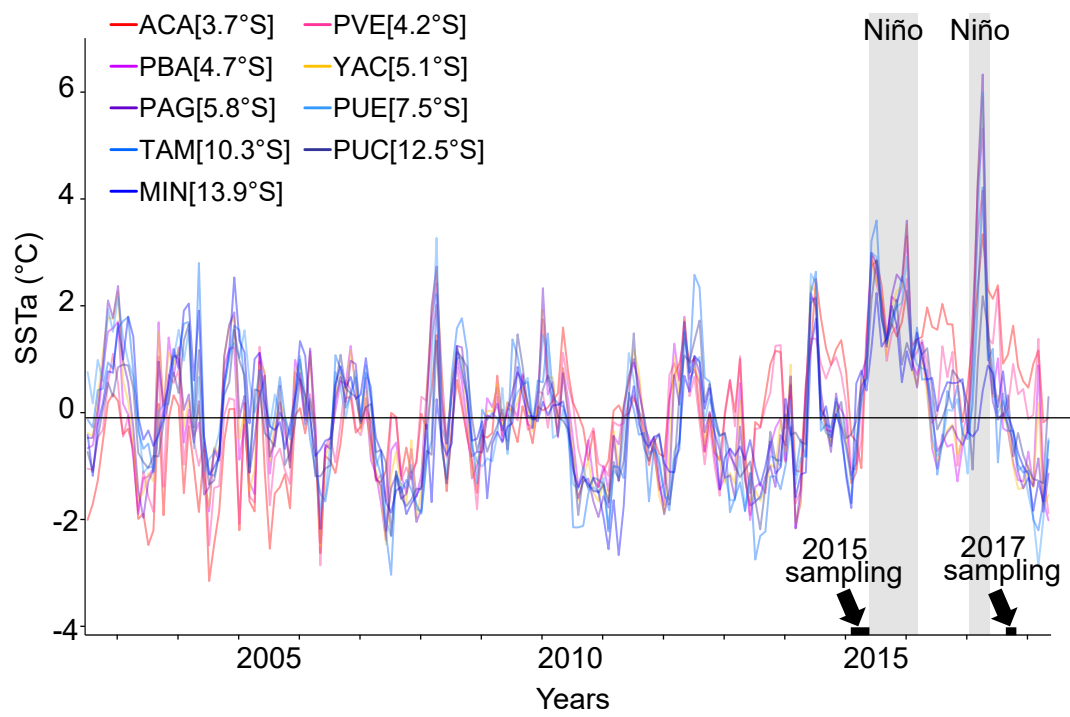


Figure 3

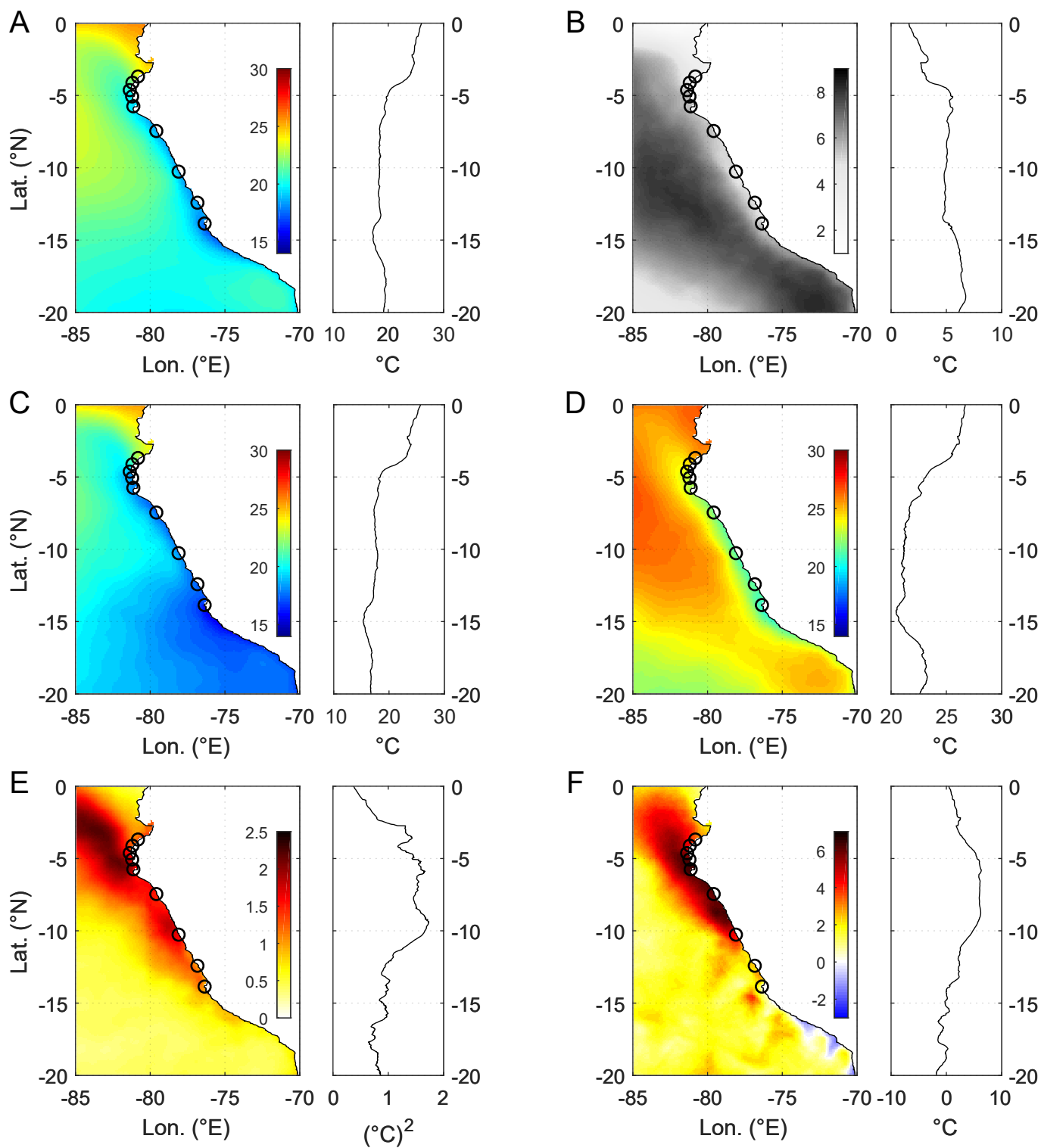


Figure 4

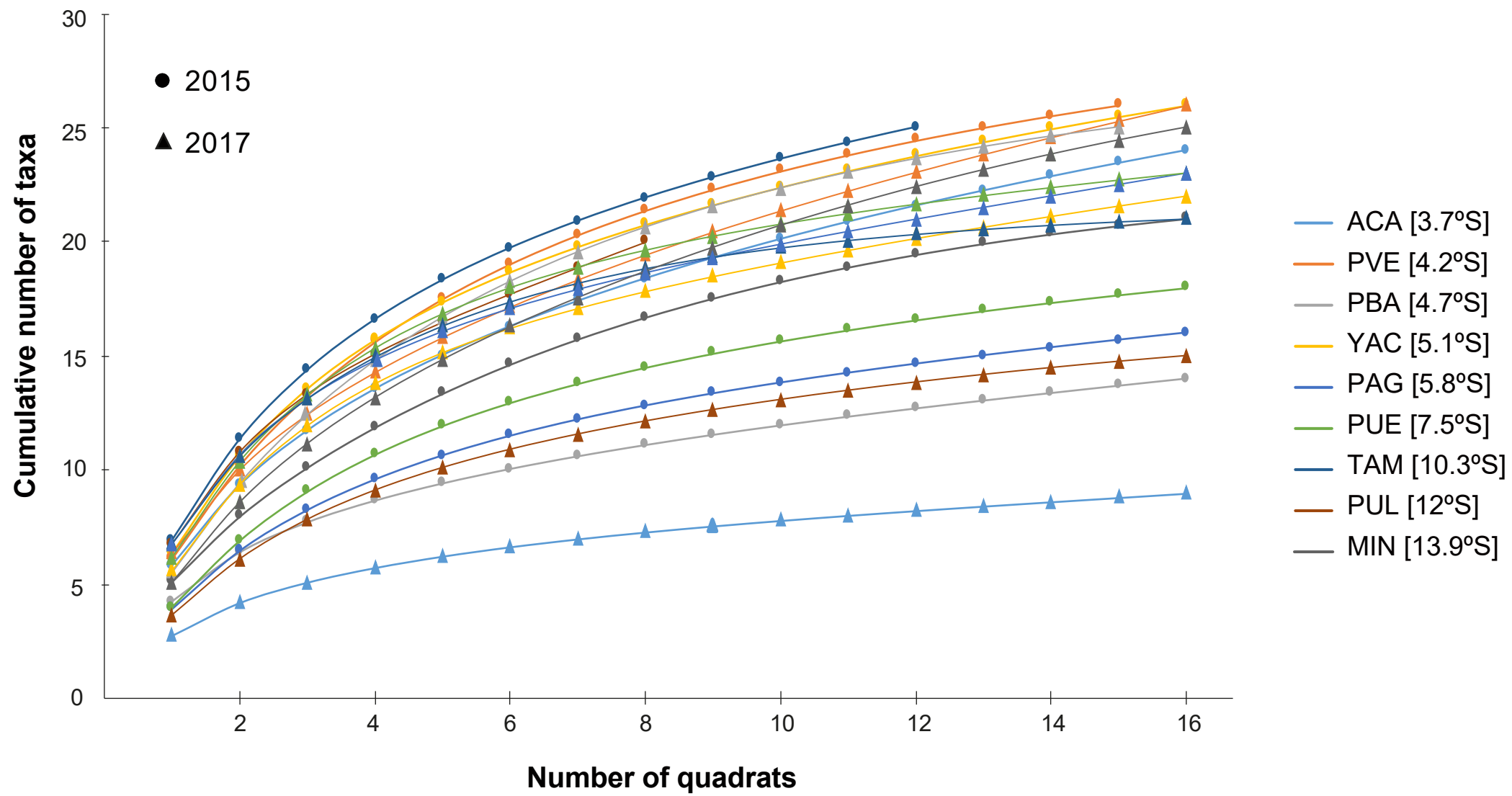


Figure 5

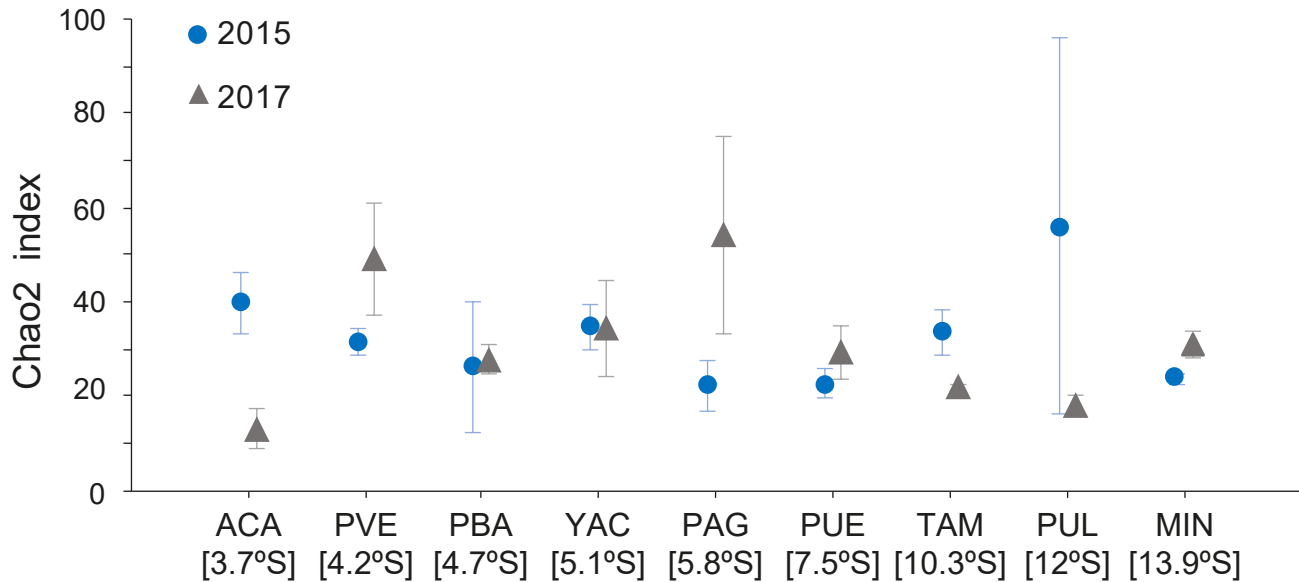


Figure 6

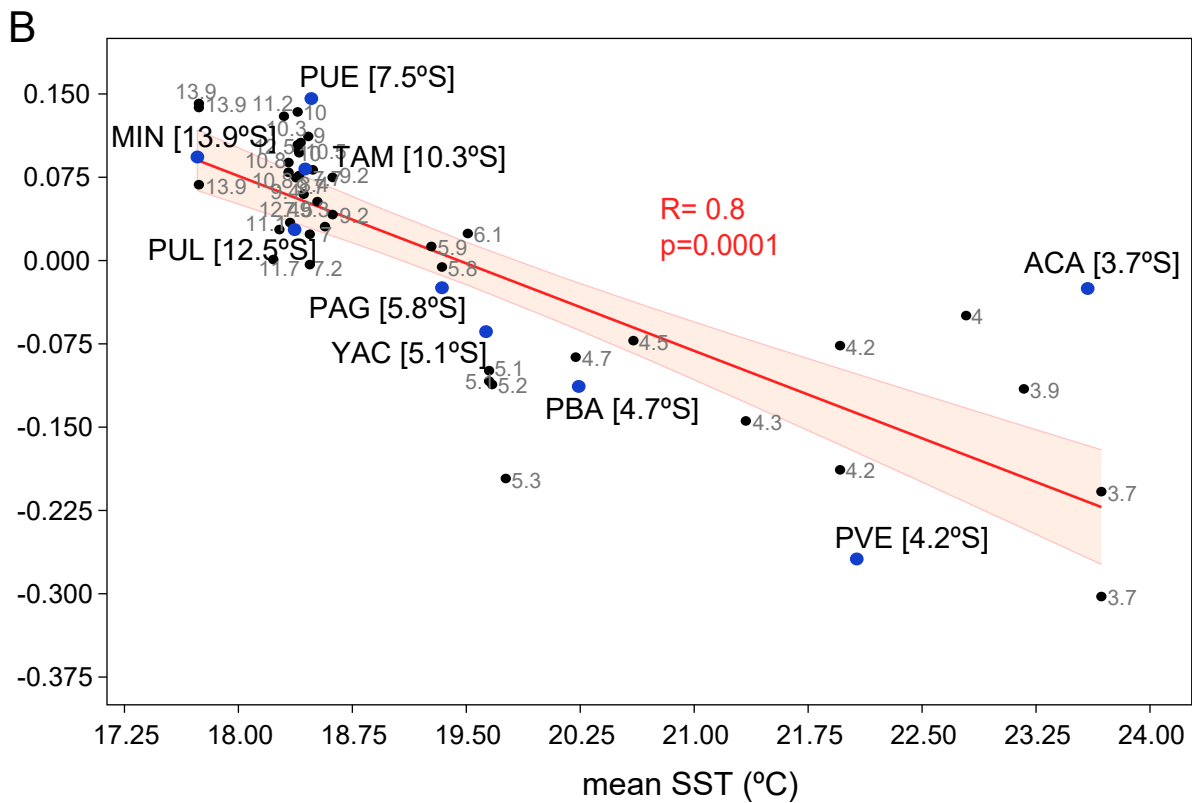
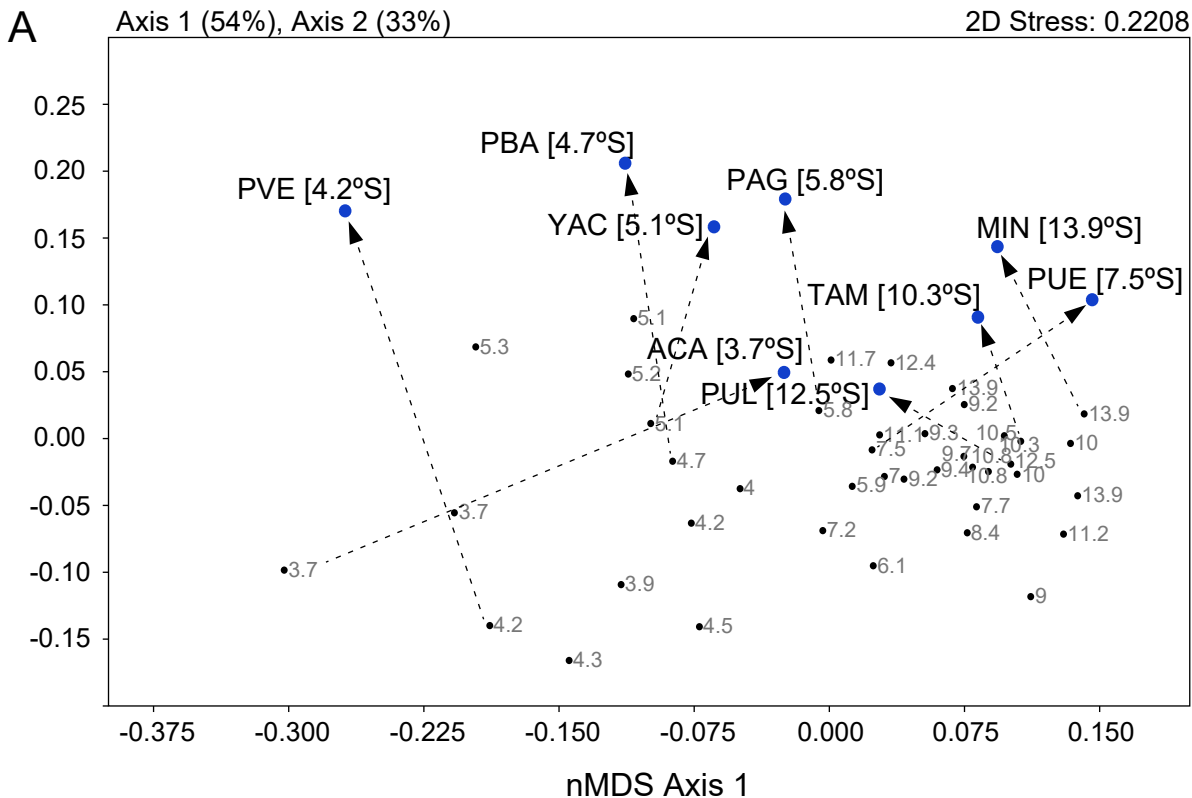


Figure 7

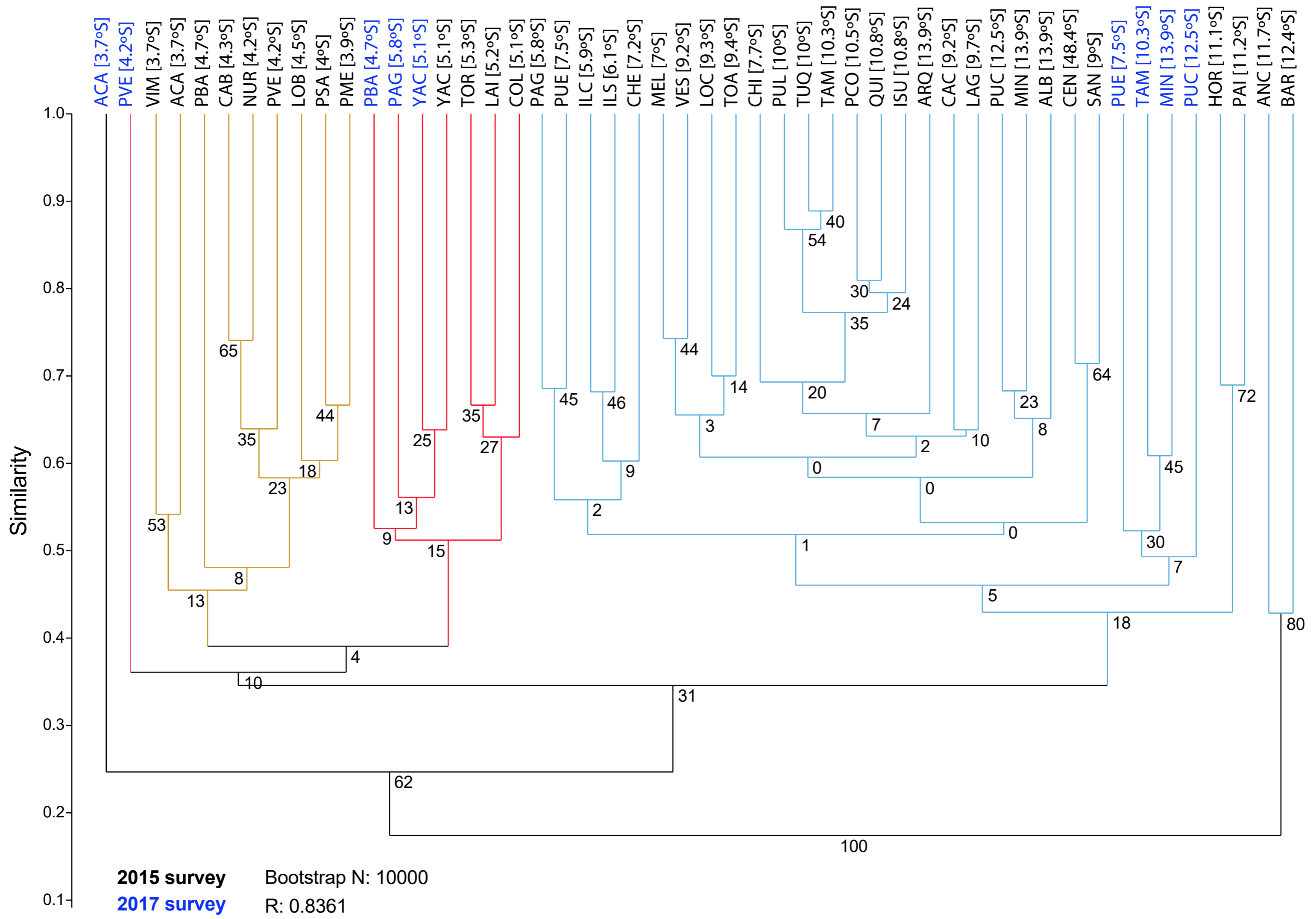


Figure 8

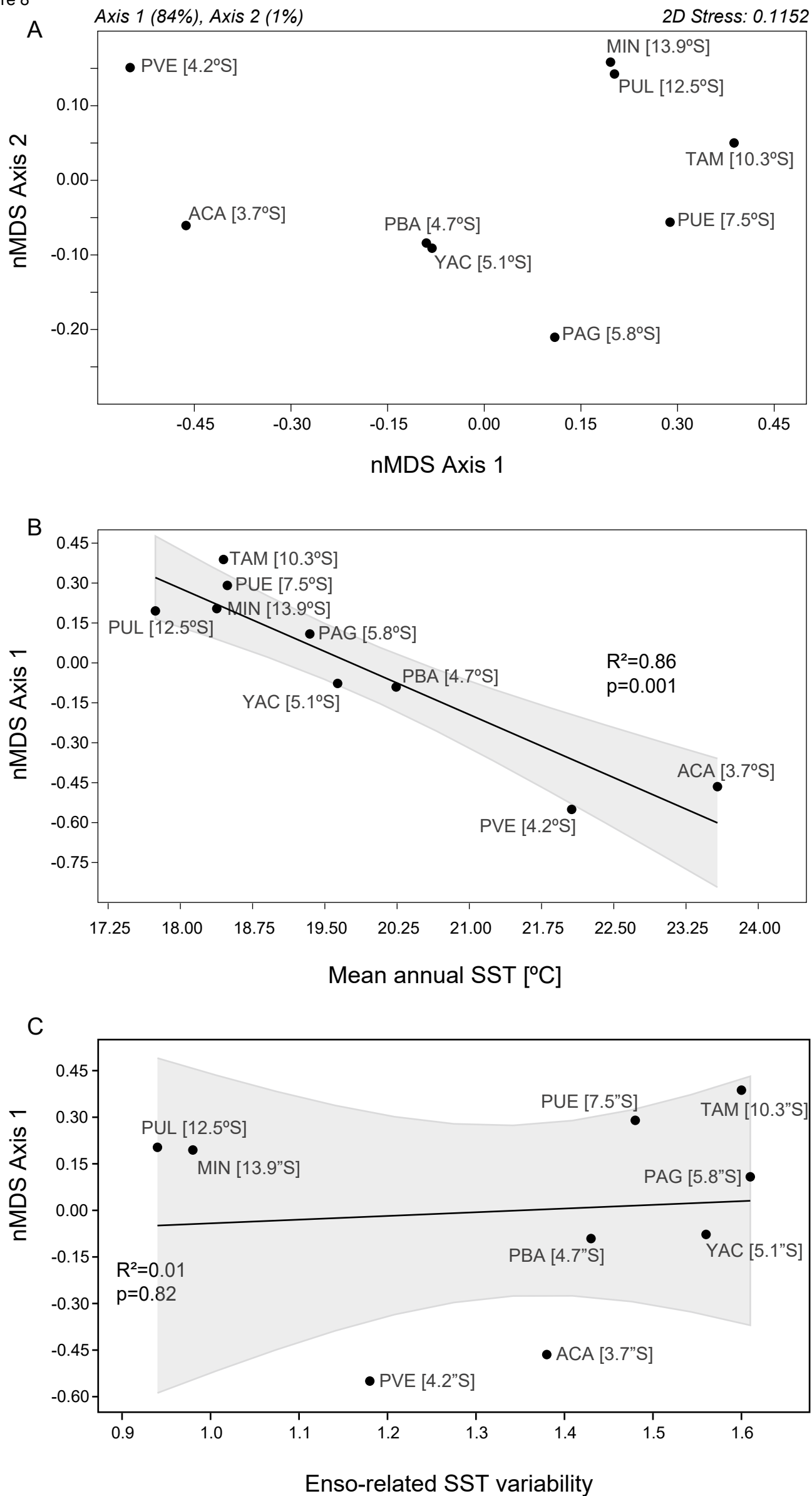
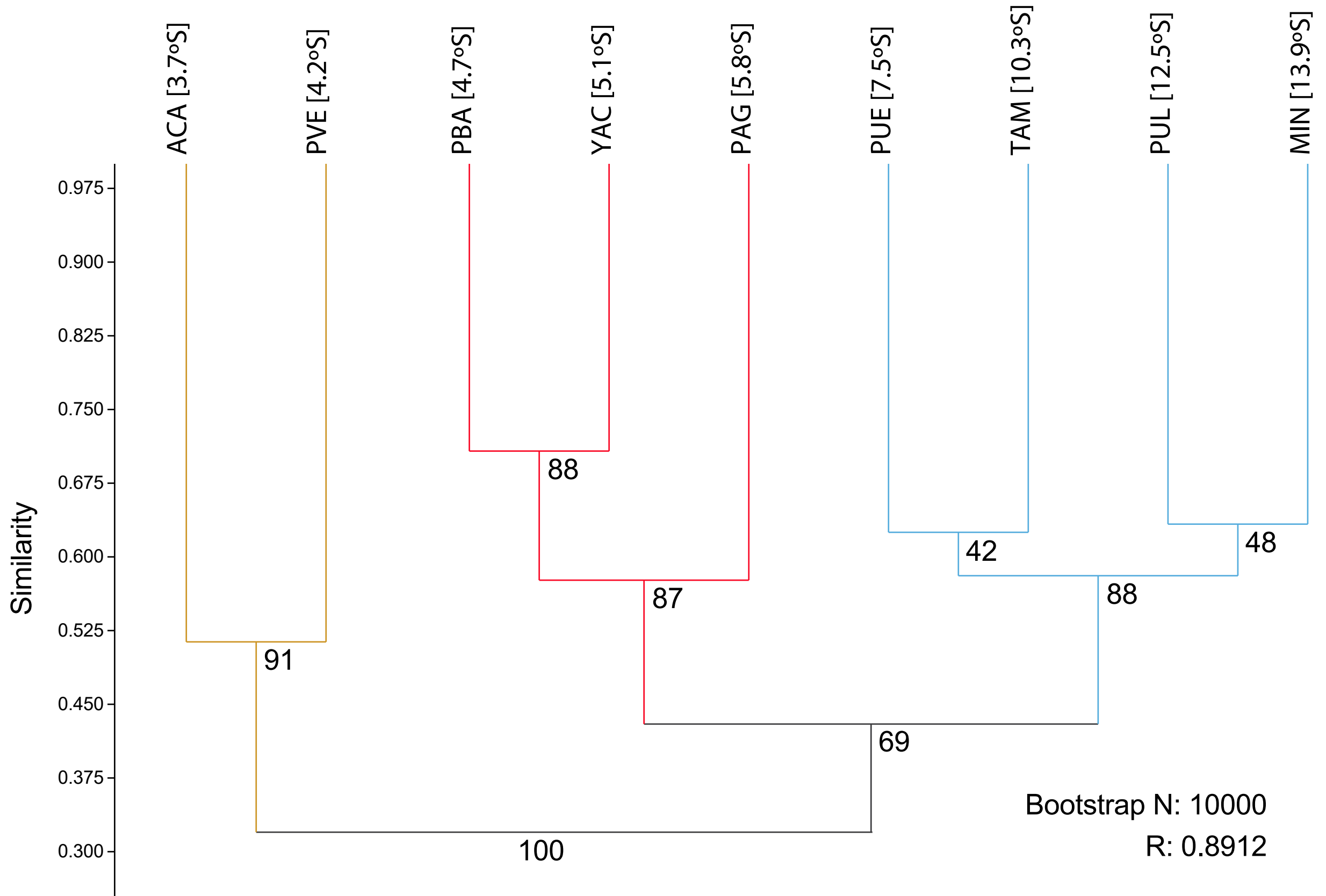


Figure 9



Declaration of interests

The authors declare that they have no known competing financial interests or personal relationships that could have appeared to influence the work reported in this paper.

The authors declare the following financial interests/personal relationships which may be considered as potential competing interests:

AUTHORSHIP STATEMENT

Manuscript title: Changes in rocky intertidal communities after the 2015 and 2017 El Niño events along the Peruvian coast

All persons who meet authorship criteria are listed as authors, and all authors certify that they have participated sufficiently in the work to take public responsibility for the content, including participation in the concept, design, analysis, writing, or revision of the manuscript. Furthermore, each author certifies that this study has not been and will not be submitted to or published in any other publication before its appearance in *Estuarine, Coastal and Shelf Science*.

Authorship contributions

Category 1

Conception and design of study: J. Valqui, A. Pacheco, B. Ibañez-Erquiaga, M. Carré;

acquisition of data: J. Valqui, B. Ibañez-Erquiaga, Lynn Wilbur, A. Indacochea, J. Avila-Peltroche, M. Pérez-Huaranga;

analysis and/or interpretation of data: J. Valqui, D. Ochoa, M. Carré, A. Pacheco, B. Ibañez-Erquiaga.

Category 2

Drafting the manuscript: J. Valqui, M. Carré;

revising the manuscript critically for important intellectual content: A. Pacheco, B. Ibañez-Erquiaga, D. Ochoa, J. Cardich, R. Salas-Gismondí, A. Pérez, A. Indacochea, J. Avila-Peltroche, M. Rivera Ch..

Category 3

Approval of the version of the manuscript to be published (the names of all authors must be listed):

J. Valqui, B. Ibañez-Erquiaga, A. S. Pacheco, L. Wilbur, D. Ochoa, J. Cardich, M. Pérez-Huaranga, R. Salas-Gismondí, A. Pérez, A. Indacochea, J. Avila-Peltroche, M. Rivera Ch, M. Carré

Acknowledgements

All persons who have made substantial contributions to the work reported in the manuscript (e.g., technical help, writing and editing assistance, general support), but who do not meet the criteria for authorship, are named in the Acknowledgements and have given us their written permission to be named. If we have not included an Acknowledgements, then that indicates that we have not received substantial contributions from non-authors.

This statement is signed by all the authors (a photocopy of this form may be used if there are more than 10 authors):

Author's name (typed)	Author's signature	Date
Juan Valqui		26.08.2020
Bruno Ibañez-Erquiaga		24/08/2020
Aldo S. Pacheco		24/08/2020
Lynn Wilbur		26/08/2020
Diana Ochoa		23/08/2020
Jorge Cardich		23/08/2020
Maria Pérez-Huaranga		26/08/2020
Rodolfo Salas-Gismondi		26/08/2020
Alexander Pérez		23/08/2020
Aldo Indacochea		24/08/2020
Jose Avila-Peltroche		23/08/2020
Maria Rivera Ch		26/08/2020
Matthieu Carré		23/08/2020



Click here to access/download
Supplementary Material
Table_S1_abundance.xlsx





Click here to access/download
Supplementary Material
Table_S2_Incidence.xlsx





[Click here to access/download](#)

Supplementary Material

[Valqui et al_ECSS_Supplementary information.docx](#)

